치의과학박사 학위논문

The molecular basis for anti-cancer activity of EGFR inhibitor afatinib in oral cancer

구강암에서 EGFR 저해제인 Afatinib의

항암 효능 및 새로운 분자기작에 관한 연구

2023년 8월

서울대학교 대학원

치의과학과 구강병리학전공

한 정 민

The molecular basis for anti-cancer activity of EGFR inhibitor afatinib in oral cancer

지도교수 조 성 대

이 논문을 치의과학 박사학위논문으로 제출함

2023년 6월

서울대학교 대학원

치의과학과 구강병리학전공

한 정 민

한정민의 치의과학 박사학위논문을 인준함

2023년 7월

위 원 장 _____ 노 상 호 _____ (인)

부위원장 _____ 홍 성 두 _____ (인)

위 원 _____ 안 상 건 _____ (인)

위 원 _____ 윤 혜 정 _____ (인)

위 원 _____ 조 성 대 _____ (인)

Abstract

The molecular basis for anti-cancer activity of EGFR inhibitor afatinib in oral cancer

Jung-Min Han

Oral Pathology major

The Graduate School

Seoul National University

(Directed by Professor Sung-Dae Cho, D.V.M., Ph.D.)

Objective: Afatinib has been shown in numerous studies to have anti-cancer effects against various types of cancers including oral cancer by irreversibly inhibiting the tyrosine kinases of the ErbB family proteins.

However, the precise underlying mechanism of afatinib on oral cancer is still poorly understood. Thus, this study aimed to explore the molecular mechanism underlying the anti-cancer properties of afatinib in oral cancer.

Methods: *In silico* analysis using databases like The Cancer Genome Atlas (TCGA), Gene Expression Omnibus (GEO), and Clinical Proteomic Tumor Analysis Consortium (CPTAC) along with immunohistochemistry (IHC) staining, were carried out to look into the expression patterns of EGFR and Mcl-1 and analyze their correlation in oral cancer. To investigate the anti-cancer efficacy of afatinib and its molecular mechanism, various *in vitro* and *in vivo* tests were performed, including trypan blue exclusion assay, western blotting analysis, 4′-6-diamidino-2-phenylindole (DAPI) staining, flow cytometric analysis, Quantitative real time PCR (qPCR), mitochondrial membrane potential assay, construction of an over-expression vector, transient transfection, and a tumor xenograft model.

Results: In a computer simulation and IHC staining, I found that the expression levels of the epidermal growth factor receptor (EGFR) and the myeloid cell leukemia-1 (Mcl-1) were higher in head and neck cancer (HNC) patients compared to normal tissues and high expression of EGFR

and Mcl-1 was strongly linked to poor prognosis in HNC patients. The EGFR inhibitor, afatinib suppressed cell viability and induced apoptosis in the HSC-3, SAS, and Ca9.22 cell lines, which showed relatively higher expression and correlation between two proteins compared to other cancer cell lines. It effectively downregulated Mcl-1 protein expression without altering mRNA expression. Overexpressing Mcl-1 using transient transfection reduced the anti-proliferative and pro-apoptotic effects of afatinib on cell lines. Afatinib significantly increased the expression of Bim_{EL}, a downstream target of Mcl-1, resulting in a decrease in mitochondrial outer membrane permeabilization (MOMP) and release of cytochrome c into the cytosol. Afatinib also leads to a reduction in the activation of the mTOR signaling pathway such as p-p70S6 and p-4E-BP1 in oral cancer cell lines. I confirmed the importance of mTOR in afatinib-induced apoptosis using MHY1485 (an mTOR activator) and rapamycin (an mTOR inhibitor). Afatinib demonstrated superior anti-proliferative and pro-apoptotic effects in oral cancer cell lines compared to gefitinib, a first-generation TKI, and effectively decreased the Mcl-1 protein expression. In addition, the anti-cancer activity of afatinib was confirmed in a xenograft mouse model bearing HSC-3 cell line.

Conclusion: Taken together, these findings show that afatinib induces

apoptosis in human oral cancer through altering the EGFR/mTOR/Mcl-1 axis, clearly suggesting its potential as an anti-neoplastic chemotherapeutic candidate for the treatment of oral cancer.

Keywords: Oral cancer, Afatinib, Apoptosis, Epidermal Growth Factor Receptor, Myeloid cell leukemia-1, Mammalian target of rapamycin

Student Number: 2019-36435

Table of contents

Review of literature

The epidermal growth factor receptor (EGFR) is a transmembrane receptor that plays a crucial role in cell growth, differentiation, and survival [1]. The EGFR family comprises four unique members that share common structural components, including EGFR (also known as HER1 or ErbB1), ErbB2 (also called HER2 or neu), ErbB3 (also referred to as HER3), and ErbB4 (also known as HER4). Binding of the ligand to EGFR results in the activation of inactive receptors through either homo- or hetero-dimerization [2]. Activation of the intracellular tyrosine kinase domain of the receptors and subsequent auto-phosphorylation initiate multiple downstream signaling pathways, including the PI3K/AKT/mTOR, STAT, and RAS/RAF/MEK pathways [3]. EGFR is highly expressed in over 90% of head and neck squamous cell carcinomas (HNSCCs). Activation of the EGFR signaling pathway is linked to a cancerous cell phenotype, suppression of apoptosis, promotion of angiogenesis, and heightened metastatic capability [4]. International guidelines recommend anti-EGFR agents as the preferred first-line treatment for patients with advanced EGFR mutations, based on their superior safety and efficacy compared to standard chemotherapy [5]. Monoclonal antibodies and small-molecule tyrosine kinase inhibitors (TKIs) represent two crucial pharmacological strategies in the field of anti-EGFR therapies [6]. Anti-

EGFR monoclonal antibodies function as competitive inhibitors that selectively bind to the inactive extracellular domain of EGFR receptors and hinder ligand-induced EGFR tyrosine kinase activation [7]. Small-molecule EGFR TKIs compete with ATP in a reversible or irreversible manner to bind the intracellular tyrosine kinase domain of EGFR, which results in the inhibition of EGFR auto-phosphorylation and downstream signaling pathways [8]. The kinase domain of EGFR is primarily encoded by exon 18 to 24, with the majority of activating mutations found in the ATP-binding pocket. Mutations such as L858R substitution in exon 21 and deletion of exon 19 are predictive markers for treatment with EGFR TKIs. The first-generation TKIs, erlotinib and gefitinib, have shown promising clinical responses in patients with these mutations, but secondary drug resistance often occurs after approximately one year of treatment. The most common resistance mechanism is the T790M mutation in exon 20, which is referred to as the gatekeeper mutation [9]. Afatinib, as a second-generation TKI, acts as a covalent, irreversible inhibitor targeting members of the ErbB family, including ErbB2 and ErbB4 [10]. Multiple prior studies have demonstrated the moderate efficacy of afatinib in patients who have developed acquired resistance to first-generation tyrosine kinase inhibitors [11, 12]. Recent data has revealed that the occurrence of the EGFR T790M acquired resistance

mutation is equally common in patients treated with afatinib as it is in patients treated with erlotinib or gefitinib [13]. As a result, third-generation EGFR TKIs, including osimertinib, targeting the T790M mutation, have been developed and are being utilized as effective second-line treatment options for many patients initially treated with afatinib [14]. In summary, EGFR plays a critical role in cancer development and progression, and targeting EGFR has emerged as a promising strategy for cancer therapy. Understanding the molecular mechanism of how Afatinib effectively inhibits EGFR activity can be an effective strategy for cancer treatment.

1. Introduction

Oral cavity is a complex organ responsible for functions such as speech, chewing, swallowing, and breathing. Although less common than other cancers, accounting for approximately 2% of all malignancies worldwide [15], oral cancer can cause significant functional and aesthetic impairment, leading to social and psychological problems that can dramatically reduce the patient's quality of life [16]. Despite the development of various treatment methods, including early detection techniques, surgical procedures, radiation therapy, and chemotherapy, oral cancer is still known to have a poor prognosis with a 5-year survival rate of less than 50%. Chemotherapeutic drugs such as cisplatin and docetaxel are currently used to treat oral cancer, but clinical problems have been reported due to systemic toxicity and drug resistance [17]. Therefore, research into the identification of critical target proteins for the development or inhibition of oral cancer and the elucidation of mechanisms involved is essential to overcome these limitations.

Epidermal growth factor receptor (EGFR) is a transmembrane receptor tyrosine kinase (RTK) with a molecular weight of 170kDa, a member of the human epidermal growth factor receptor (HER) family, and the earliest identified growth factor [18]. EGFR is divided into extracellular and intracellular regions based on the cell membrane. The extracellular region

contains four subdomains. Subdomains I and III play a role in forming the ligand-binding pocket, while II and IV are involved in the dimerization of EGFR through disulfide bonds [19]. Within the cell, there are several domains, including the juxtamembrane domain, phosphorylation domain, and C-terminal domain. Binding of ligands such as epidermal growth factor (EGF) and transforming growth factor-α (TGF-α) to EGFR leads to the formation of homo- or heterodimers with other members of the EGFR or HER family, resulting in conformational changes in EGFR [20]. The heterodimers of EGFR induced by ligands promote autophosphorylation of multiple tyrosine residues in the cytoplasmic domain. Phosphorylated tyrosine residues activate downstream signaling pathways, which then interact with various adapter and signaling molecules involved in cell growth and proliferation [21]. EGFR is frequently overexpressed in solid tumors of epithelial origin, and has been studied as a target for tumor therapy. In oral cancer, EGFR overexpression is associated with poor prognosis, treatment resistance, and lower patient survival rates, likely due to dysregulation or mutation during cancer development and progression [4].

The two main strategies for targeting EGFR are antibody blockade and inhibition of tyrosine kinase activity using TKIs [22]. The chimeric anti-EGFR monoclonal antibody cetuximab was the first to be developed and

works by blocking ligand binding to inhibit overexpressed EGFR. First-generation TKIs, such as gefitinib and erlotinib, have also been used to treat oral cancer by competitively and reversibly binding to the ATP-binding site of EGFR [23]. However, despite their initial efficacy, these drugs eventually show limited efficacy due to the emergence of drug resistance, mainly caused by the T790M mutation located in exon 20 of EGFR. This mutation results in the substitution of methionine for threonine at position 790, which is an important residue for regulating inhibitor specificity in the ATP binding pocket and has been designated as a 'gatekeeper'. The T790M mutation enhances the affinity of the ATP binding pocket for ATP, thus successfully competing with the TKIs and conferring resistance to these drugs [24]. Other mechanisms of resistance, such as amplification of HER2 and MET oncogenes or histological transformation to small cell carcinoma, have also been proposed but are less frequent. Despite attempts to overcome this with combined-target therapy using radiation or chemotherapy, it has been reported that effective EGFR inhibition responses are not observed [25, 26]. The development of irreversible TKIs, such as Afatinib, has provided a promising solution to overcome the limitations of first-generation TKIs. Afatinib was approved by the FDA in 2013 as a first-line treatment for locally advanced or metastatic non-small cell lung cancer patients with EGFR

mutations, making it the first irreversible ErbB family inhibitor used as a first-line therapy [27]. This highly potent TKI binds covalently to the ATP-binding site of EGFR and remains bound until the drug effect is eliminated. Clinical trials have demonstrated its anti-tumor effects in various solid tumors, including oral cancer [28]. The use of irreversible TKIs represents a significant advancement in EGFR-targeted therapy and holds great potential for improving the treatment outcomes of patients with oral cancer.

Myeloid cellleukemia-1 (Mcl-1), a member of the Bcl-2 family with anti-apoptotic properties, has been demonstrated to promote cell survival by inhibiting apoptosis [29]. Mcl-1 is known to be highly expressed in solid tumors, as well as in patients with hepatocellular carcinoma, pancreatic cancer, testicular cancer, cervical cancer, non-small cell lung cancer, melanoma, and ovarian cancer [30, 31]. Several studies have reported an association between increased Mcl-1 expression and adverse clinical outcomes [32, 33], and recent research has shown that Mcl-1 upregulation is closely linked to the activation of EGFR signaling pathways, such as AKT/mTOR and MEK/ERK [34, 35]. However, compared to studies on other prevalent cancers, research on the correlation between EGFR expression and the expression of the representative oncoprotein, Mcl-1, as well as the signaling mechanisms involved in oral cancer, is significantly

lacking. Therefore, further investigation is needed to fully understand the complex interactions between EGFR and Mcl-1 in oral cancer and to develop more effective treatment strategies targeting both molecules.

The purpose of this study is to demonstrate the correlation between EGFR and Mcl-1 expression in oral cancer patients, to prove the inhibitory effect of the second-generation TKI, afatinib, on oral cancer, and to newly elucidate the signaling mechanisms of afatinib in regulating Mcl-1 expression as an EGFR-targeted therapeutic agent in HSC-3, SAS, and Ca9.22 oral cancer cell lines.

2. Materials and methods

2.1 The Cancer Genome Atlas (TCGA) database

The TCGA database (https://portal.gdc.cancer.gov/) was used to access and analyze the HNC dataset. The process of trimming data was done using Jupyter Notebook and Pandas with Python 3.0, and the code is available at https://github.com/kunalchawlaa/TCGA-Oral-Cancer. FPKM-UQ files were used to analyze the correlation of mRNA expression between EGFR and Mcl-1 in HNC (n=369) and compare and evaluate the EGFR mRNA expression levels between normal (n=32) and tumor (n=369) samples.

2.2 Gene Expression Omnibus (GEO) database

The GEO (https://www.ncbi.nlm.nih.gov/geo/), a public genomics database, was used for the analysis of EGFR and Mcl-1 mRNA expression in HNC. Variation in EGFR mRNA levels was examined within the same cases by comparing adjacent non-tumor epithelium (n=40) and cancer (n=40) using the GEO series GSE37991 reporter identifier ILMN_2376484. Using the GEO series GSE31056, the differences in EGFR (1956_at) mRNA levels between the normal (n=24), margin (n=49), and cancer (n=23) groups were analyzed. The differences in EGFR mRNA levels between the normal (n=45), dysplasia (n=17), and cancer (n=167) groups were assessed using the GEO

series GSE30784 reporter identifier 201983_s_at. Mcl-1 mRNA levels were assessed in normal (n=45), dysplasia (n=17), and cancer (n=167) groups using the GEO series GSE30784 with reporter identifiers 200796_s_at, 200797_s_at, 200798_x_at, and 214056_at, to determine the variation in expression between these groups. To ensure consistency and accuracy, all extracted data was normalized using Geo2R.

2.3 Clinical Proteomic Tumor Analysis Consortium (CPTAC) database

Proteogenomic analyses for a wide range of cancer types are available in The CPTAC database (https://pdc.cancer.gov/pdc/). Reporter ion intensity log2 ratio unshared peptides of EGFR and Mcl-1 was displayed for comparison of expression levels between normal samples (n=33) and tumor samples (n=57).

2.4 Cancer Cell Line Encyclopedia (CCLE) database

After evaluation of clinical databases, the cell line database (https://portals.broadinstitute.org/ccle) was reviewed. EGFR and Mcl-1 mRNA levels were analyzed in correlation with EGFR and Mcl-1 copy number values using data from upper aerodigestive cell lines.

2.5 Kaplan-Meier (KM) Plotter survival analysis

Overall survival (OS) rate was analyzed in HNC patients according to the expression levels of EGFR and Mcl-1 using the online survival analysis software KM plotter (http://kmplot.com/analysis).

2.6 Clinical tissue samples

Between 2006 and 2007, the Department of Oral and Maxillofacial Surgery at Seoul National University Dental Hospital (Seoul, Republic of Korea) collected 52 tissues from patients who had undergone surgical treatment for oral cancer. These tissues were then subjected to IHC staining in a retrospective study. This study received approval from the Institutional Review Board (IRB) of Seoul National University Dental Hospital (IRB No. ERI20021).

2.7 Immunohistochemistry (IHC) staining

Paraffin-embedded tissues from oral cancer patients were sectioned at 4 μm thickness for this study. The paraffin was melted by holding the sections at 60°C for 1 hour, followed by washing with neo-clear and graded ethanol to rehydrate the specimens. For antigen retrieval, the sections were microwaved in antigen retrieval citrate buffer (pH 6.0) for 10 minutes, and then treated

with peroxidase blocking reagent (Dako, Carprinteria, CA, USA) for 5 minutes to inactivate endogenous peroxidase activity. Sections were incubated overnight at 4°C in a humidified chamber with a primary antibody against p-EGFR (Cat. No. 3777; 1:100), Mcl-1 (Cat. No. 39224; 1:50), and c-caspase3 (Cat. No. 9664; 1:1000). The next day, the sections were reacted with REALTM EnVisionTM/horseradish peroxidase (HRP) Rabbit/Mouse (Dako) for 30 minutes at room temperature (RT), followed by a color reaction with REALTM DAB and Chromogen with Substrate Buffer (Dako) for 30 seconds. The sections were then counterstained with hematoxylin, dehydrated, and mounted with Permount solution (Thermo Fisher Scientific, Waltham, MA, USA).

2.8 Evaluation of IHC staining

Immunohistochemically stained sections were semi-quantitatively evaluated by two pathologists. Tumor cells showing cytoplasmic staining were regarded as positive cells. The intensity of staining (0, negative; 1, weak; 2, moderate; and 3, strong) and the percentage of positive cells (0, 0%; 1, 1%–9%; 2, 10%–49%; 3, 50%–100%) were scored. The final immunohistochemical scores were established by multiplying the intensity and the percentage scores. The final scores ≥6 and ≥2 were classified as

high expression and those <6 and <2 as low expression for p-EGFR and Mcl-1, respectively.

2.9 EGFR mutation analysis

The genomic DNA from oral cancer cells was isolated using InstaGene Matrix (Bio-Rad Laboratories, Hercules, CA, USA) method. EGFR exon 20 was amplified with the following primers: sense 5'-GTA AAA CGA CGG CCA GT-3', antisense 5'-GCG GAT AAC AAT TTC ACA CAG G-3'. PCR amplification was carried out over a total of 35 cycles (for 30 seconds at 95°C, 30 seconds at 58°C, and 1 minute at 72°C). The PCR products were purified using ExoSAP-IT (Thermo Fisher Scientific, Waltham, MA, USA), and the samples were Sanger sequenced using an Applied Biosystems ABI PRISM 3730XL Analyzer.

2.10 Cell culture and reagents

Human oral keratinocyte (HOK) cell line was obtained from Lifeline cell technology (Oceanside, CA, USA). HSC-2, HSC-3, HSC-4, SAS and Ca9.22 cell lines were kindly provided by Hokkaido University (Hokkaido, Japan). HN22 and MC-3 cell lines were kindly provided by Dankook University (Cheonan, Republic of Korea) and Fourth Military Medical University (Xi'an,

China), respectively. HO-1-N1 and HO-1-U1 cell lines were purchased from the Japanese Collection of Research Bioresources Cell Bank (Osaka, Japan). YD-10B, YD-15, YD-15M cell lines were purchased from the Korean Cell Line Bank (Seoul, Republic of Korea). The HOK cell line was grown using DermaLife K Keratinocyte Medium Complete Kit (Lifeline Cell Technology). The HN22, HSC-2, HSC-3, HSC-4, SCC-9, SAS, Ca9.22, HO-1-N1, HO-1-U1 and MC-3 cell lines were maintained in Dulbecco's modified Eagle's medium (DMEM)/nutrient mixture F-12 (WELGENE, Gyeongsan, Republic of Korea). The YD-10B, YD-15 and YD-15M cell lines were cultured in Roswell Park Memorial Institute (RPMI) 1640 medium (WELGENE). The culture media used for all cell lines were supplemented with 10% fetal bovine serum (FBS) and 1% penicillin/streptomycin (P/S), and the cells were maintained at 37°C in a humidified atmosphere with 5% CO_2. The cells were rinsed with Dulbecco's phosphate-buffered saline (DPBS). Afatinib (BIBW2992), gefitinib (ZD1839), and MHY 1485 were purchased from Selleck Chemicals, and rapamycin was obtained from Sigma-Aldrich. The chemical compounds were dissolved in dimethyl sulfoxide (DMSO) and aliquoted, then stored at -20°C.

2.11 Trypan blue exclusion assay

Cells were dissociated from the culture plate using a 0.25% trypsin-EDTA solution (WELGENE), and then resuspended in 1 mL of PBS. A solution of 0.4% trypan blue (Gibco, Paisley, Scotland, UK) was applied to the cells for staining, and a CytoSMART automatic cell counter (Corning, Tewksbury, MA, USA) was used to determine the number of viable cells in the sample. Only trypan blue-unstained cells were counted as viable.

2.12 Western blotting

A 1X RIPA lysis buffer (Millipore Corp, Burlington, MA, USA) in combination with phosphatase inhibitor tablets (Thermo Scientific Inc., Rockford, IL, USA) and protease inhibitor cocktails (Roche, Mannheim, Germany) was used to extract total protein from human oral cancer cell lines. The protein concentration of each sample was determined using a DC Protein Assay Kit (BIO-RAD Laboratories, Madison, WI, USA). An equal amount of protein from each sample was then heated with 5X protein sample buffer at 95 °C for 10 minutes, separated by SDS-PAGE and transferred to immunoblot PVDF membranes. After blocking with 5% skim milk in Tris-buffered saline with Tween 20 (TBST) for 1.5 hours at RT, the membranes were incubated with the specified primary antibodies at 4°C overnight. After washing, the membranes were incubated for 2 hours at RT with the appropriate secondary

antibodies (1:3000, catalog #: GTX213110–01 or GTX213111–01, GeneTex Inc., Irvine, CA, USA) conjugated to HRP. Immunoreactive protein bands were detected using either x-ray film or the Image Quant LAS 500 system (GE Healthcare Life Sciences, Piscataway, NJ, USA) with WestGlow™ FEMTO chemiluminescent substrate (BIOMAX, Seoul, Republic of Korea). ImageJ software was used to calculate protein levels. The following primary antibodies were used in the experiment. Rabbit anti-human polyclonal antibodies against c-PARP (Cat. No. 9541; 1:1000), c-caspase-3 (Cat. No. 9664; 1:1000), p-mTOR (Cat. No. 2971; 1:1000), p-p70S6 (Cat. No. 9205; 1:1000), p-eIF4E (Cat. No. 9741; 1:1000), Bim (Cat. No. 2819; 1:1000), Mcl-1 (Cat. No. 4572; 1:1000), and rabbit anti-human monoclonal antibodies against p-EGFR (Cat. No. 3777; 1:1000), mTOR (Cat. No. 2983; 1:1000), and p-4E-BP1 (Cat. No. 2855; 1:1000) were purchased from Cell Signaling Technology, Inc (Danvers, MA, USA). Rabbit anti-human polyclonal antibody against EGFR (Cat. No. sc-03; 1:1000), goat anti-human polyclonal antibody against t-Bid (Cat. No. 34325; 1:1000), and mouse anti-human monoclonal antibodies against β-actin (Cat. No. 47778; 1:3000) and GAPDH (Cat. No. ab9484; 1:3000) were purchased from Santa Cruz Biotechnology, Inc (Santa Cruz, CA, USA).

2.13 4′-6-diamidino-2-phenylindole (DAPI) staining.

A DAPI solution (Sigma-Aldrich) was used to examine changes in the nuclear morphology of apoptotic cells. Cells were seeded onto 60 mm^2 plates and treated with 8μM of afatinib for 24 hours. Following the treatment, the cells were collected, washed twice with PBS, and then fixed with 100% methanol RT for 10 minutes. The cells were then washed again with PBS, seeded onto glass slides coated with a layer of the substance, and stained with a DAPI solution (2 μg/ml). Changes in cell morphology were visualized and analyzed using a fluorescence microscope.

2.14 Annexin V/ Propidium iodide (PI) staining.

The presence of apoptosis was assessed using a FITC Annexin V apoptosis detection kit (BD Pharmingen, San Jose, CA, USA). The harvested cells were rinsed twice with PBS and then exposed to Annexin V-FITC and PI dyes for 15 minutes at RT. The stained cells were then examined using a FACS Caliber instrument and the resulting measurements were calculated using Cell Quest software (BD Biosciences).

2.15 Quantitative real time PCR (qPCR).

Mcl-1 mRNA levels were quantified by qPCR analysis. After obtaining the target cDNA, PCR was performed using AMPIGENE qPCR Green Mix Hi-Rox (Enzo Life Sciences, Inc). The qPCR was performed using the StepOne Plus Real-Time PCR System. The qPCR was carried out using the StepOne Plus Real-Time PCR System (Applied Biosystems, CA, USA) and the target cDNA was amplified using the following primers: sense 5'-GTA TCA CAG ACG TTC TCG TAA GG-3', antisense 5'-CCA CCT TCT AGG TCC TCT ACA T-3' for Mcl-1 and sense 5'- GTG GTC TCC TCT GAC TTC AAC-3', antisense 5'- CCT GTT GCT GTA GCC AAA TTC-3' for GAPDH. The Mcl-1 and GAPDH amplification was carried out over a total of 40 cycles (for 2 minutes at 95℃, for 10 seconds at 95℃, and for 30 seconds at 60℃). PCR amplification was performed in triplicate for each sample, and the relative expression of Mcl-1 mRNA was determined using the 2-ΔΔCt.

2.16 Mitochondrial membrane potential (ΔΨm) assay

The change in ΔΨm was evaluated using a MitoScreen assay kit (BD Pharmingen). After harvesting, the cells were rinsed twice with PBS and then exposed to JC-1 staining solution for 15 minutes at 37℃. The cells were rinsed twice with 1X assay buffer and the JC-1 fluorescence was measured by flow cytometry.

2.17 Construction of Mcl-1 over-expression vector and transient transfection.

Open reading frame of the human Mcl-1 gene (NM_021960) was obtained by cDNA amplification with a pair of primers. The primer sequences are as follows: Mcl-1 sense 5′-GAA TTC ATG TTT GGC CTC AAA AGA-3′ (containing an EcoRI site) and Mcl-1 antisense 5′-GAA TTC CTA TCT TAT TAG ATA TGC-3′ (containing an EcoRI site). The PCR product was then ligated into a pGEM®-T Easy Vector System (Promega, Madison, WI, USA) for cloning. The target genes of interest were successfully inserted into the multiple cloning site (MCS) of the pcDNA3.1 (+) vector (Invitrogen, Carlsbad, CA, USA). The HSC-3, SAS and Ca9.22 cell lines were used for the transfection experiments. Cells were transfected with either an empty pcDNA3.1 vector or a pcDNA3.1-Mcl-1 vector construct (0.5 μg) using Lipofectamine 2000 Reagent (Invitrogen) as the transfection agent, according to the manufacturer's instructions.

2.18 Nude mouse xenograft assay

Six-week-old male BALB/c-nude mice were obtained from JA BIO, Inc. The mice used in the study were treated according to the guidelines of the

CHA University Institutional Animal Care and Use Committee (IACUC) (IACUC approval number: 230040). A fixed number of HSC-3 cells were transplanted subcutaneously into the flanks of the mice. For the tumor bearing mice, the vehicle control and afatinib (50 mg/kg/day) were orally by gavage 5 times a week for 21 days starting approximately 7 days after the start of the experiment (day 0). Tumor volume and body weight of the mice were measured twice weekly and tumor weight was measured on the day of necropsy. The volume of the tumor was determined by measuring its diameter along two axes using calipers, and then calculating the volume using the formula $V = \pi/6\{(D + d)/2\}$, where D is the larger diameter and d is the smaller diameter.

2.19 Histopathological Examination of Organs

Mice organs (liver and kidney) were fixed in 10% neutral buffered formalin. Tissue sections were cut at a thickness of 4 μm and stained with hematoxylin and eosin. Histopathological changes were analyzed under a Olympus BX43 microscope.

2.20 Statistical analysis

For *in silico* studies, a paired or unpaired two-tailed Student's *t*-test was used to compare EGFR and Mcl-1 expression between normal and cancerous tissues. Spearman's rank correlation analysis was used to examine the relationship between DNA copy number and mRNA expression levels. *In vitro* studies utilized a two-tailed Student's *t*-test to assess the significance of differences between two experimental groups, and a one-way ANOVA analysis was performed for multiple comparisons using Tukey's post hoc test. Non-parametric Mann-Whitney tests were used to analyze non-normally distributed data sets in the *in vivo* studies. Pearson chi-square test was performed to analyze the association between the immunohistochemical expression of Mcl-1 and p-EGFR in oral cancer tissue samples. Data analysis was performed with GraphPad Prism version 8.4 and evaluated with SPSS 25 (SPSS, Chicago, IL, USA). All experiments were conducted independently in triplicate. The results with $P < 0.05$ were defined as statistically significant.

3. Results

3.1 EGFR expression is frequently upregulated and is significantly associated with poor prognosis in HNC patients.

I performed an *in silico* analysis to assess the expression of EGFR in human HNC, with the aim of investigating its clinical significance in human pathogenesis. The present study first used the CCLE database to confirm the correlation between gene copy number and EGFR mRNA expression in HNC and found a positive correlation between the two (Figure 1A). Using the GEO datasets (GSE31056 1956_at and GSE30784 201983_s_at) and TCGA database, I compared the EGFR mRNA expression levels between HNC tissues and normal tissues, and found a significant increase in EGFR mRNA expression levels in HNC tissues compared to normal tissues (Figure 1B-1D). I also analyzed the GEO dataset (GSE37991 ILMN_1755535) and revealed significantly elevated EGFR mRNA expression level in 40 pairs of HNC tissues compared to adjacent non-tumor epithelium (Figure 1E). By utilizing the CPTAC database, I observed a significant increase in EGFR protein expression levels in HNC tissues compared to normal tissues (Figure 1F). Using the KM Plotter, a significant correlation was found between EGFR expression and the overall survival (OS) rate in patients with HNC, indicating that high levels of EGFR expression lead to a poor OS rate in these patients

(Figure 1G). These results indicate that EGFR may function as a diagnostically significant malignant factor in human HNC and be associated with poor prognosis in patients.

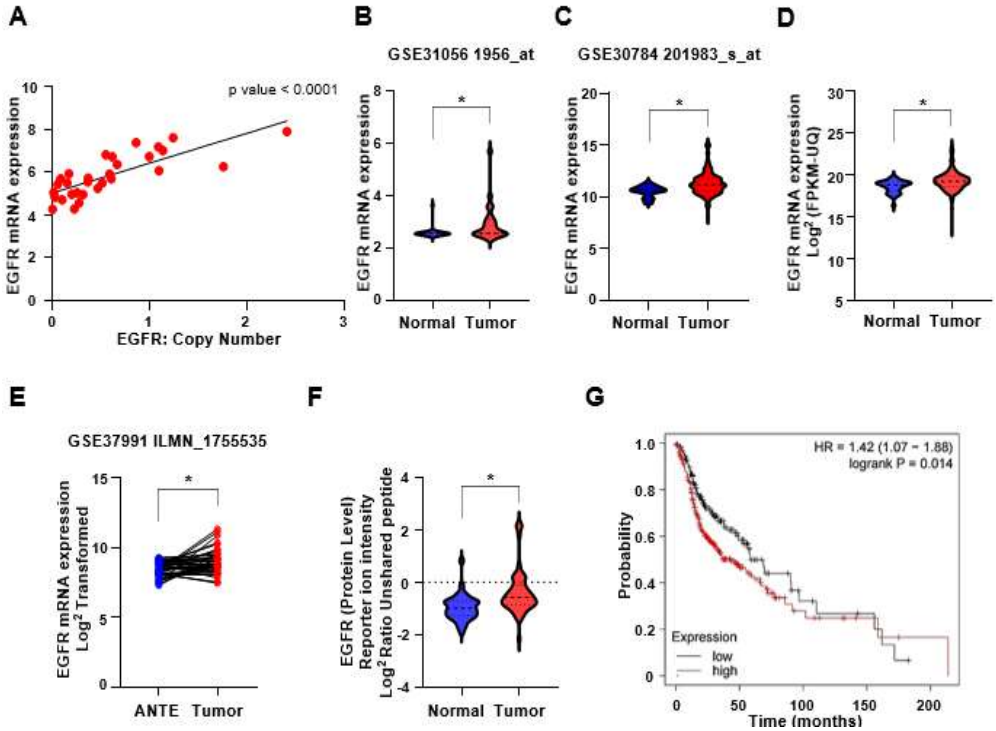

Figure 1. EGFR expression and prognosis in human HNC. (A) The association between EGFR gene copy number and mRNA levels was analyzed using the CCLE database. Comparison of EGFR mRNA expression levels between HNC tissues and normal tissues using GEO datasets (B, C) and the TCGA database (D). (E) Analysis of EGFR mRNA expression levels in HNC tissues and adjacent normal epithelium tissues using GEO dataset. (F) Evaluation of EGFR protein expression levels in HNC tissues and normal tissues using the CPTAC database. (G) Evaluation of the association between EGFR protein expression levels and poor overall survival in HNC patients using the KM Plotter Analysis.

3.2 Mcl-1 expression is widely expressed in human HNC and is significantly linked to poor patient prognosis.

An analysis of the GEO dataset (GSE30784 200796_s_at, GSE30784 200797_s_at, GSE30784 200798_x_at, and GSE30784 214056_at) revealed that Mcl-1 mRNA expression levels were elevated in comparison to normal tissue (Figures 2A-2D). Using the CPTAC database, Mcl-1 protein expression was found to be significantly higher in HNC compared to normal tissues (Figure 2E). The relationship between Mcl-1 expression and the OS in HNC patients was examined using the KM plotter, and showed that high levels of Mcl-1 expression were significantly associated with a poor OS in these patients (Figure 2F). Based on these results, it is suggested that Mcl-1 could play a crucial role as a diagnostic marker for malignancy in human HNC, and its expression may be associated with unfavorable prognostic outcomes in patients.

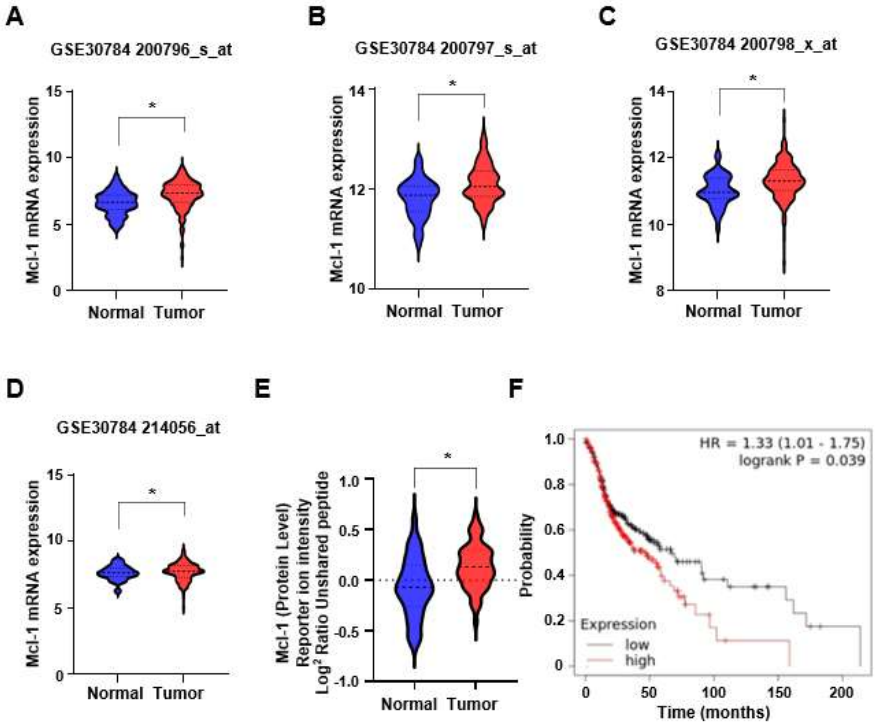

Figure 2. Mcl-1 expression and prognosis in human HNC. (A-D) Comparison of Mcl-1 mRNA expression levels between HNC tissues and normal tissues using GEO datasets. (E) Analysis of Mcl-1 protein expression levels in HNC tissues and normal tissues using the CPTAC database. (F) Evaluation of the association between Mcl-1 protein expression levels and poor overall survival in HNC patients using the KM Plotter Analysis.

3.3 EGFR expression is directly proportional to Mcl-1 expression in human HNC, and these expression patterns are closely correlated with patient prognosis.

To investigate the correlation between EGFR and Mcl-1 mRNA expression levels in HNC, the TCGA database was used, and a positive correlation was found (Figure 3A). It was also found that the co-expression high levels of EGFR and Mcl-1 showed a significant association with poor prognosis in HNC patients, compared to other group (Figure 3B). These results indicate a correlation between EGFR and Mcl-1 expression levels in human HNC, and suggest that high levels of expression for these factors are associated with a higher likelihood of poor prognosis in patients.

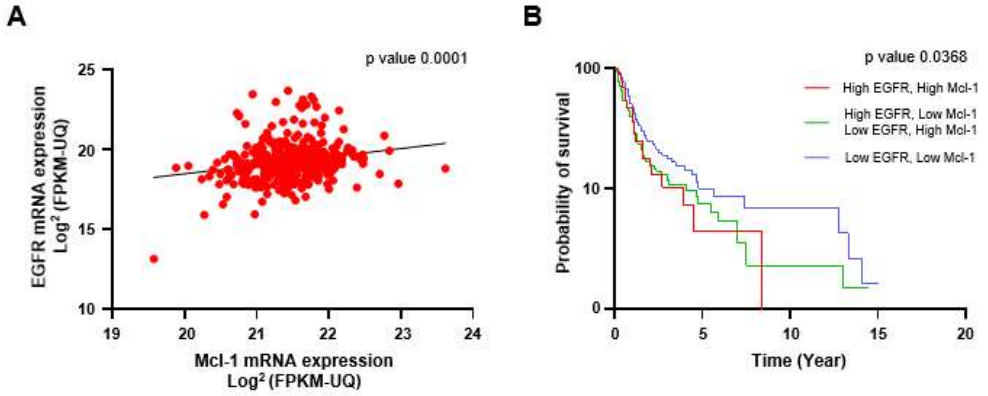

Figure 3. The correlation between EGFR and Mcl-1 expression and prognosis in human HNC. Using the TCGA database to analyze the correlation between EGFR and Mcl-1 expression (A), and their impact on patient prognosis (B).

3.4 Strong association between p-EGFR and Mcl-1 proteins expression in oral cancer tissue.

Of the 52 oral cancer tissues, 42.3% (22/52) and 44.2% (23/52) showed high expression of p-EGFR and Mcl-1, respectively. p-EGFR and Mcl-1 demonstrated a similar spatial distribution within the same tissue section in p-EGFR+/Mcl-1+ cases. The expression level of p-EGFR was strongly correlated with that of Mcl-1 (Figure 4A-4C).

Taken together, these results suggest that EGFR and Mcl-1 are deeply correlated in oral cancer, and that their expression is a clinically important factors in the prognosis of oral cancer patients.

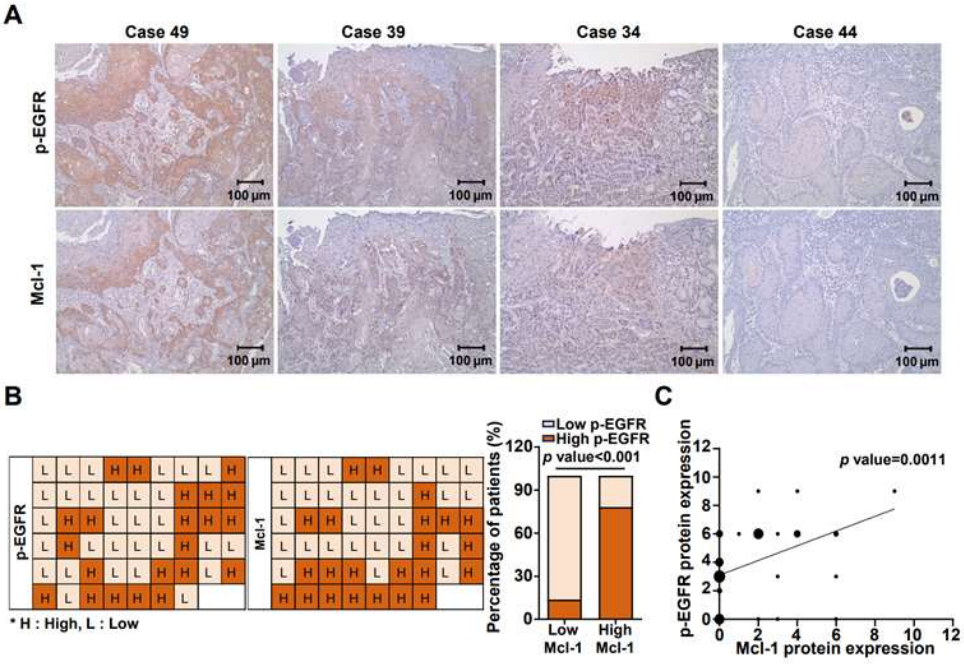

Figure 4. Correlation between the protein expression of p-EGFR and Mcl-1 in oral cancer tissues. The association between the protein expression levels of p-EGFR and Mcl-1 was demonstrated in 52 oral cancer tissues using IHC analysis. (A) The representative images of p-EGFR and Mcl-1 expression in oral cancer tissues (scale bar: 100 μm). Cases 49, 39, 34 are p-EGFR^{+}/Mcl-1^{+}, and case 44 is p-EGFR^{-}/Mcl-1^{-}. (B) The graphical pattern of p-EGFR and Mcl-1 expression using IHC scores in 52 oral cancer tissues. (C) The correlation analysis of p-EGFR and Mcl-1 expression in 52 oral cancer tissues based on IHC scores.

3.5 The expression of p-EGFR and Mcl-1 proteins in oral cancer cell lines is positively correlated.

To investigate the correlation between the expression of p-EGFR and Mcl-1 proteins in oral cancer cell lines, the protein expression levels of p-EGFR$^{(Tyr1068)}$ and Mcl-1 were analyzed by Western blotting in HOK and various oral cancer cell lines (HN22, HSC-2, HSC-3, HSC-4, SCC-9, SAS, Ca9.22, HO-1-N1, HO-1-U1, YD-10B, MC-3, YD-15, and YD-15M). Most of the oral cancer cell lines showed higher expression of p-EGFR and Mcl-1, compared to HOK, and three of them (HSC-3, SAS, and Ca9.22) showed proportionally higher expression and correlation between two proteins compared to other cancer cell lines (Figure 5). Therefore, these three cell lines were used in the following experiments. These findings suggest that the expression levels of p-EGFR and Mcl-1 may be critical factors in the development of oral cancer, especially in HSC-3, SAS, and Ca9.22 cell lines.

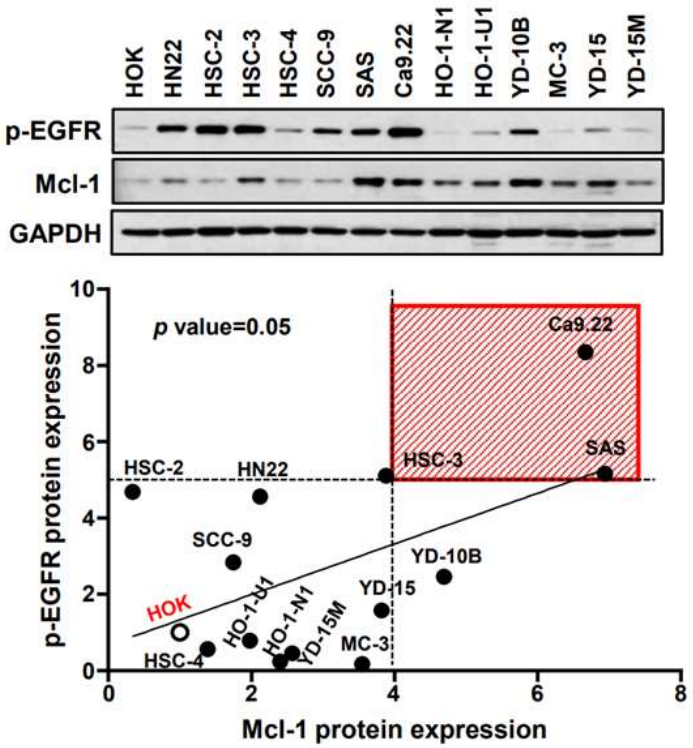

Figure 5. Correlation between the protein expression of EGFR and Mcl-1 in oral cancer cell lines. Correlation analysis between EGFR and Mcl-1 protein expression was conducted using western blotting in HOK and 13 oral cancer cell lines, and cell lines with high correlation between EGFR and Mcl-1 expression were identified (indicated by the red box). Normalization was performed using GAPDH as a control. The graph displays the means ± standard deviation (SD) of three independent experiments.

3.6 T790M mutation is not present in human oral cancer cell lines.

To determine the presence of the T790M mutation in Exon 20 of oral cancer cell lines HSC-3, SAS, and Ca9.22, genomic DNA extraction was performed followed by Sanger sequencing. The experimental results revealed the absence of the T790M mutation in HSC-3, SAS, and Ca9.22 cell lines (Figure 6). These findings suggest the suitability of pre-third-generation EGFR TKIs as potential anticancer agents for oral cancer cell lines.

Gene	Exon #	Codon	Target codon	Amino acid	Ref.	Alt.
EGFR	Exon20	790	c.2369	T790M	C	T

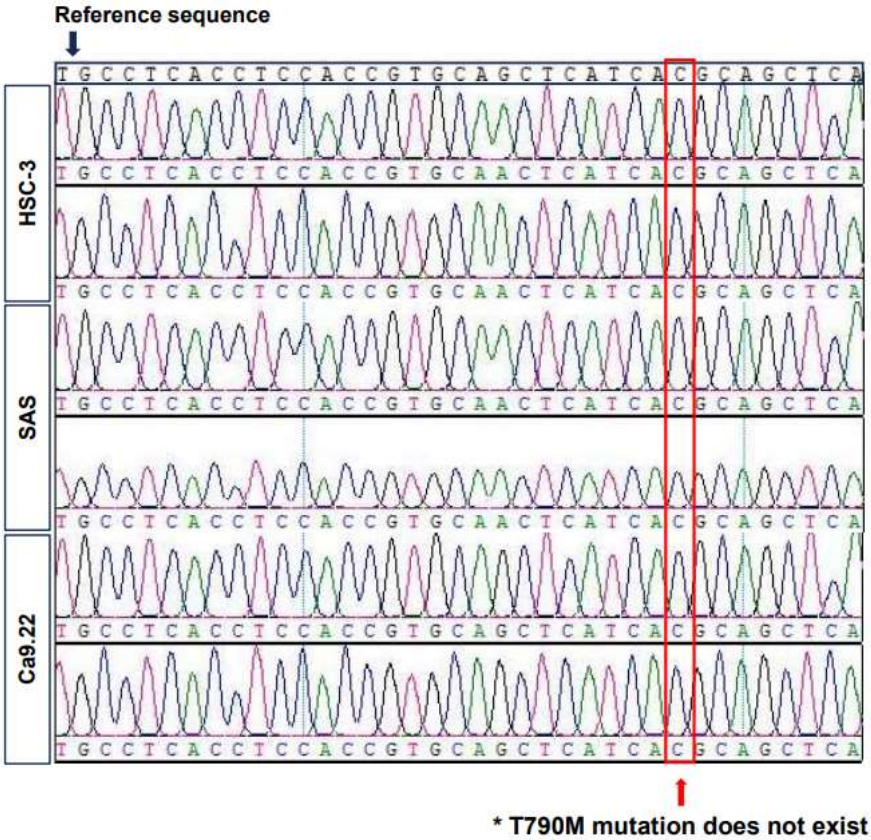

Figure 6. Presence of T790M Mutation in Human Oral Cancer Cell Lines

For the analysis of T790M mutation in exon 20 of the EGFR in oral cancer cell lines, genomic DNA extraction was performed, and PCR amplification was carried out following optimized PCR conditions. The PCR product was purified, and Sanger sequencing was conducted.

3.7 Afatinib suppresses cell viability and downregulates the expression of p-EGFR and Mcl-1 proteins in human oral cancer cell lines.

To evaluate the potential cytotoxic effect of afatinib on oral cancer cell lines, HSC-3, SAS, and Ca9.22 cell lines were treated with 8 μM afatinib and incubated for 24 hours. The cells were then subjected to a trypan blue exclusion assay. The results showed that cell viability was significantly and markedly suppressed by afatinib (Figure 7A). To investigate whether the expression of p-EGFR and Mcl-1 was effectively downregulated by afatinib in oral cancer cell lines, Western blotting was performed under the same conditions after treatment with afatinib. Statistical analysis showed that afatinib caused a significant decrease in the expression levels of both proteins (Figure 7B). To investigate the mechanism by which Mcl-1 protein is regulated by afatinib, qPCR was performed. It was found that Mcl-1 mRNA level was not affected by afatinib in any of the three cell lines (Figure 7C). These results suggest that afatinib exerts an anti-proliferative effect on human oral cancer cells by effectively reducing the levels of Mcl-1 protein.

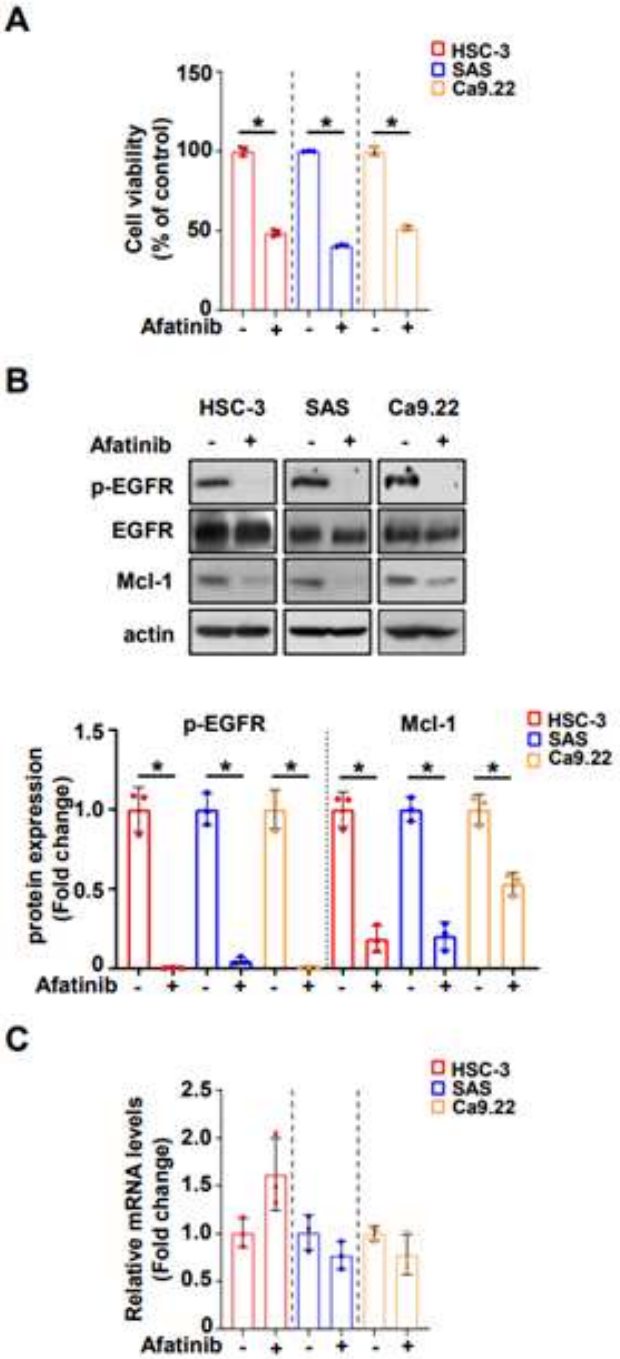
A
HSC-3
SAS
Ca9.22
Cell viability
(% of control)
150
100
50
0
Afatinib - + - + - +
B
HSC-3
SAS
Ca9.22
Afatinib - + - + - +
p-EGFR
EGFR
Mcl-1
actin
p-EGFR
Mcl-1
protein expression
(Fold change)
1.5
1.0
0.5
0
Afatinib - + - + - + - + - + - +
C
Relative mRNA levels
(Fold change)
2.5
2.0
1.5
1.0
0.5
0
Afatinib - + - + - +

Figure 7. Effect of afatinib on growth inhibition and its inhibitory effects on p-EGFR and Mcl-1 protein expression in human oral cancer cell lines. (A) HSC-3, SAS, and Ca9.22 cells were treated with afatinib (0 and 8 μM) for 24 hours and cell viability was measured using a trypan blue exclusion assay. (B) The effects of DMSO or afatinib for 24 hours on p-EGFR and Mcl-1 proteins were determined using a Western blotting. (C) Expression levels of Mcl-1 mRNA were determined using qPCR. The graph displays the means ± SD of three independent experiments. *$P < 0.05$ by two-tailed Student's *t*-test.

3.8 Afatinib induces apoptosis in human oral cancer cell lines.

To determine the type of cell death induced by afatinib, Western blotting was employed to detect PARP and caspase 3, markers of apoptosis. The cleaved caspase 3 and c-PARP were significantly elevated in response to afatinib treatment compared to the vehicle control (Figure 8A). The number of apoptotic nuclei with condensation or fragmentation was significantly increased following treatment with afatinib, as visualized by DAPI staining (Figure 8B). Annexin V/PI double staining was conducted to further confirm the apoptotic activity of afatinib. The results showed a significant increase in Annexin V-positive cells when treated with afatinib compared to the control (Figure 8C). Collectively, these findings indicate that afatinib promotes apoptotic cell death in human oral cancer cell lines.

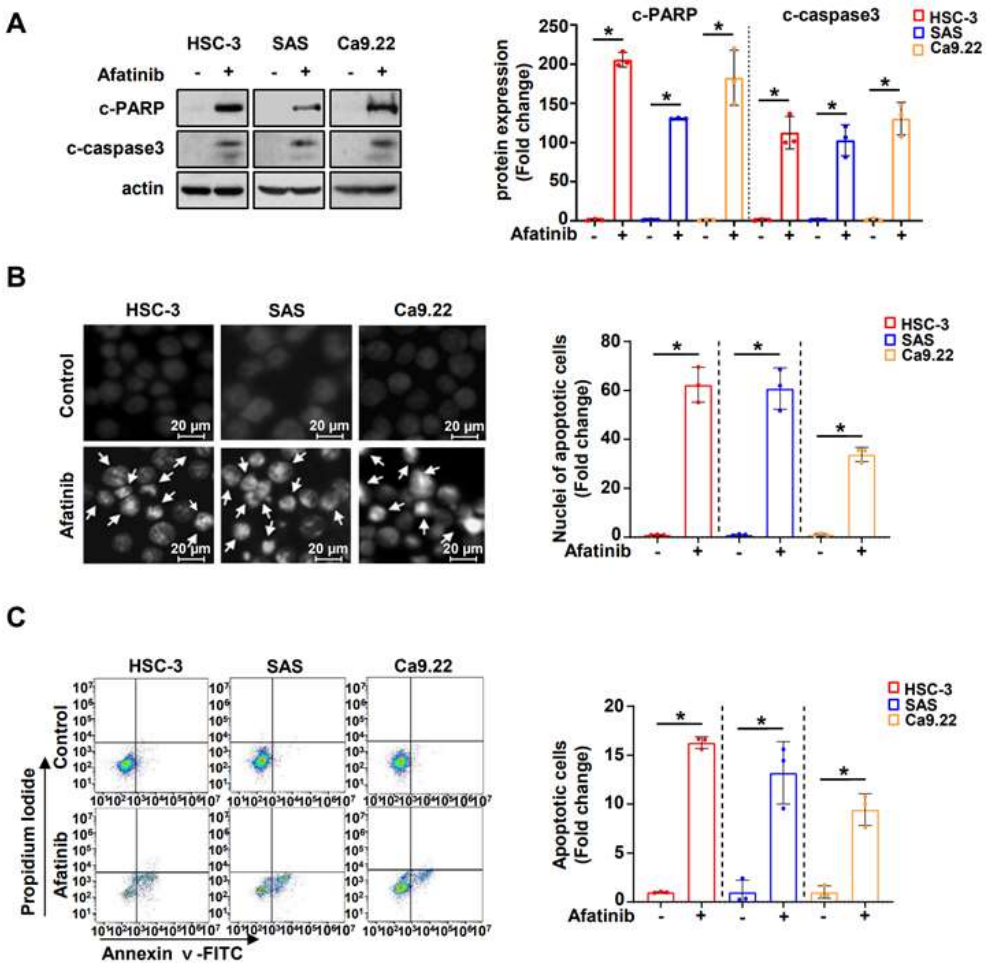

Figure 8. Effect of afatinib on apoptosis in oral cancer cell lines (A) The apoptotic effects of afatinib (0 and 8 μM) were assessed by Western blot analysis of cleaved caspase-3 and PARP. (B) Detection of apoptotic features, including chromatin condensation and nuclear fragmentation, was achieved through DAPI staining (indicated by white arrows), (scale bar: 20 μm). (C) Annexin V/PI staining was performed to measure the proportion of apoptotic

cells. The graph displays the means ± SD of three independent experiments.

*$P < 0.05$ by two-tailed Student's *t*-test.

3.9 Mcl-1 is related to afatinib-induced apotosis in oral cancer cell lines.

To determine whether afatinib-mediated apoptosis is dependent on Mcl-1, three cell lines were transfected with either an empty vector or a vector expressing Mcl-1. Overexpression of Mcl-1 significantly rescued cell viability and reversed afatinib-induced c-PARP. (Figures 9A and 9B). This finding was further corroborated by demonstrating that the proportion of apoptotic nuclei in cells overexpressing Mcl-1 was lower than in controls (Figure 9C). Furthermore, the percentages of Annexin V-positive cells in Mcl-1-overexpressing samples were reduced compared to the control, supporting the above observation (Figure 9D). These findings suggest that a key mechanism for afatinib-induced apoptosis in human oral cancer cell lines may involve the Mcl-1 protein.

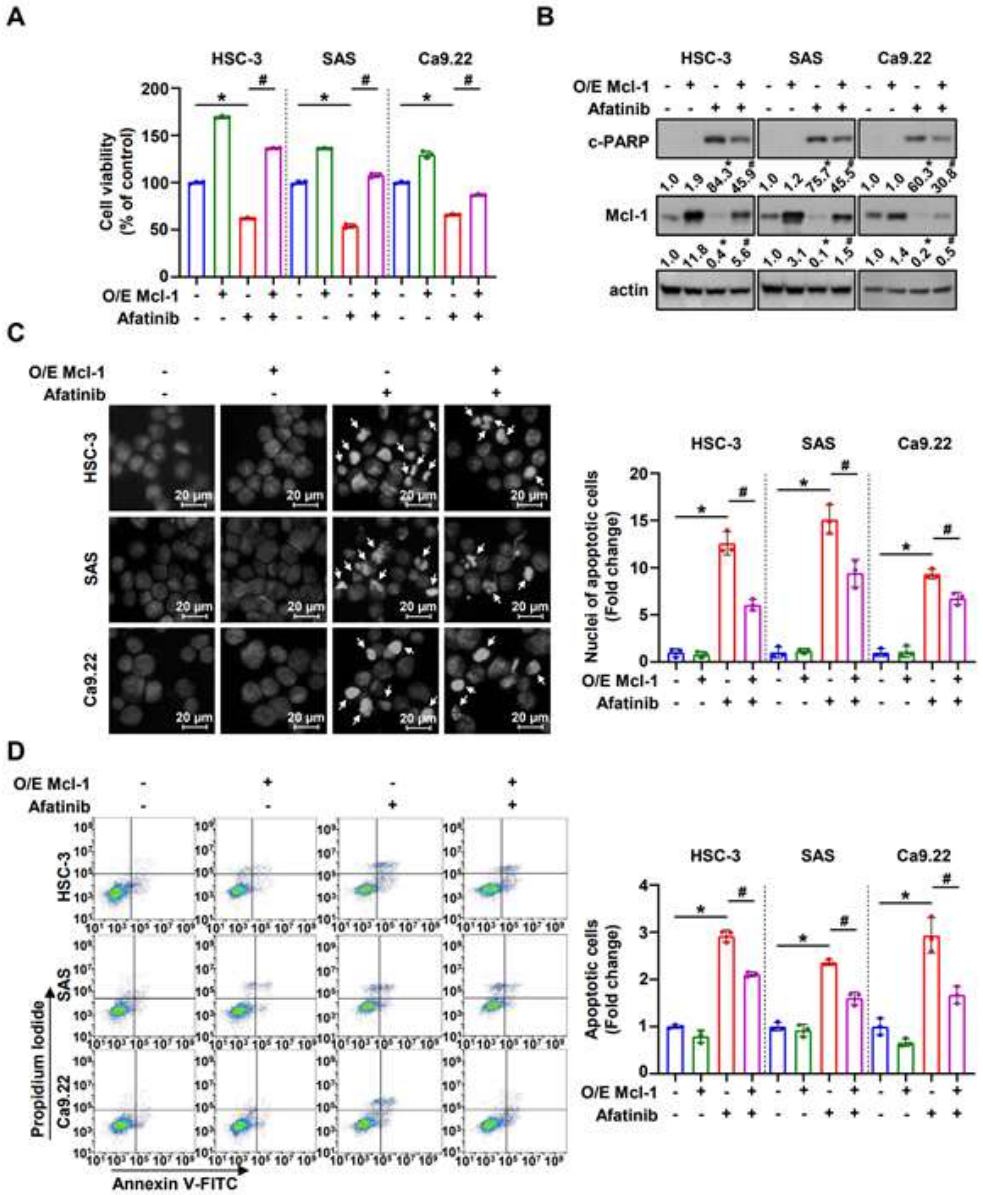

Figure 9. Apoptotic effect of afatinib through depletion of Mcl-1 protein in oral cancer cell lines. Cells were transfected with either empty pcDNA3.1 vector or pcDNA3.1-Mcl-1 plasmid (0.5 μg) and then treated with afatinib

(0 and 8 μM) for 24 hours after 6 hours of transfection. (A) Cell viability was assessed using a trypan blue exclusion assay. (B) Mcl-1 and c-PARP protein expression levels were assessed by Western blot analysis. (C) Detections of apoptotic features were identified through DAPI staining. (D) To quantify the proportion of apoptotic cells, Annexin V/PI staining was performed. The graph displays the means ± SD of three independent experiments. *P< 0.05 by one-way ANOVA.

3.10 Afatinib induces mitochondrial-dependent apoptosis in human oral cancer cell lines.

Because Mcl-1 function is known to affect BH3-only pro-apoptotic Bcl-2 family members for the mitochondrial-dependent pathway, the expression levels of Bim and t-Bid were analyzed. As shown in Figure 10, treatment with afatinib significantly increased the expression of Bim in all three cell lines. However, the expression of t-Bid was only increased in the HSC-3 and SAS cell lines, but not in the Ca9.22. To investigate whether afatinib induces apoptosis via mitochondrial dysfunction, JC-1 staining was performed. Afatinib treatment resulted in a significant reduction in red fluorescence compared to the control group, confirming that the loss of $\Delta\Psi m$ was induced by afatinib (Figure 11A). Additionally, I found that afatinib led to the release of cytochrome c into the cytosol (Figure 11B). These results indicate that afatinib induces human oral cancer cell apoptosis via mitochondrial membrane depolarization.

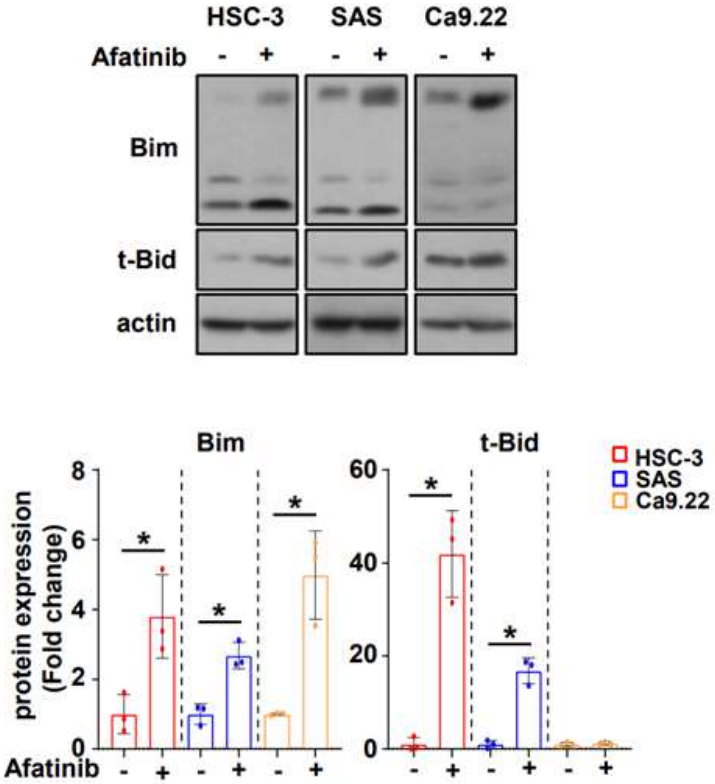

Figure 10. Effects of afatinib on the protein expression of Bcl-2 family in oral cancer cell lines. HSC-3, SAS, and Ca9.22 cells were treated with afatinib (0 and 8 μM) for 24 hours and expression levels of Bim and t-Bid, members of the Bcl-2 family of proteins, were analyzed by western blotting. The graph displays the means ± SD of three independent experiments. *$P < 0.05$ by two-tailed Student's *t*-test.

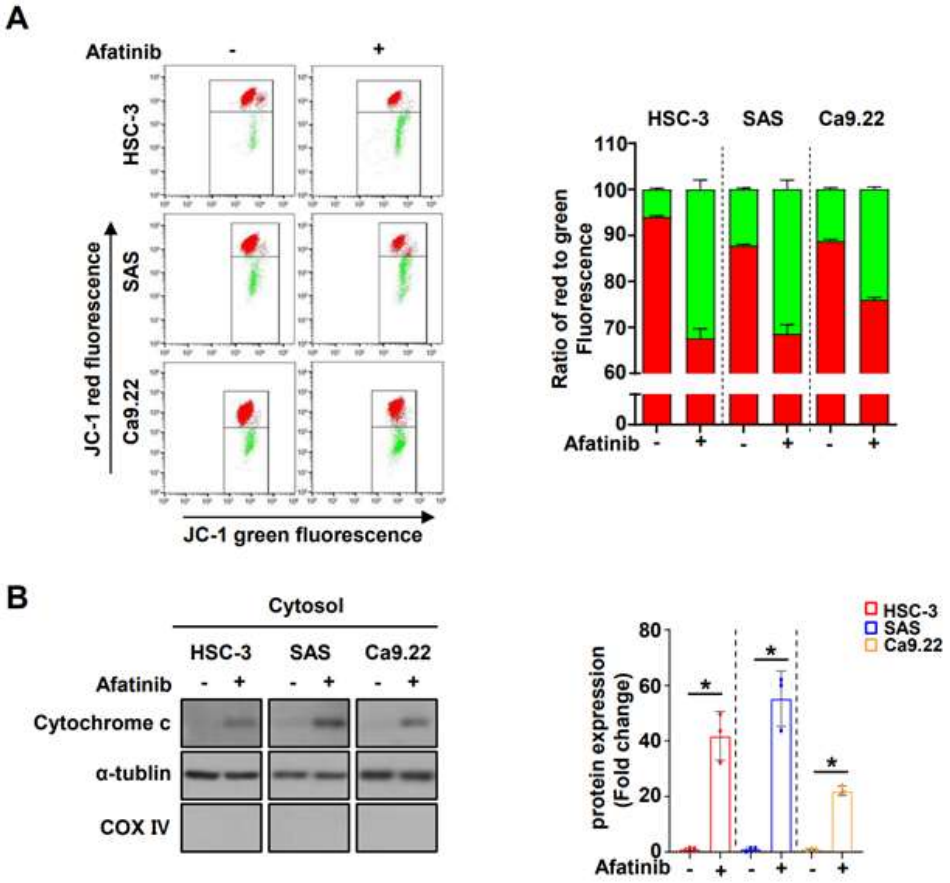

Figure 11. Effect of afatinib on mitochondria-related apoptosis in oral cancer cell lines. (A) The JC-1 assay was utilized to identify the effect of afatinib (0 and 8 μM) on mitochondrial membrane potential (DΨm). (B) Western blot analysis was performed to detect the effect of afatinib on the translocation of mitochondrial cytochrome c to the cytosol, with α-tubulin serving as a specific marker for the cytosol. Additionally, COX IV was utilized as a mitochondrial marker. The graph displays the means ± SD of three independent experiments. *$P < 0.05$ by two-tailed Student's *t*-test.

3.11 Afatinib induces apoptosis in human oral cancer cell lines by regulating the EGFR/mTOR/Mcl-1 axis.

Next, I investigated mTOR and its related proteins to determine the link between EGFR and Mcl-1 signaling by afatinib in oral cancer cell lines. Afatinib significantly reduced the expression of p-mTOR$^{(Ser2448)}$, p-P70S6K$^{(Thr389)}$, p-4E-BP1$^{(Thr37/46)}$, and p-eIF4E$^{(Ser209)}$ (Figure 12). To determine whether the Mcl-1 protein reduction and apoptotic activity induced by afatinib were an mTOR-dependent, I used MHY1485 (mTOR activator) and rapamycin (mTOR inhibitor). The expression of p-mTOR$^{(Ser2448)}$ and p-P70S6K$^{(Thr389)}$ was significantly increased in all three cell lines after treatment with MHY1485, whereas the opposite effect was observed by rapamycin (Figures 13 and 15A). The introduction of p-mTOR by MHY1485 in the HSC-3, SAS, and Ca9.22 cell lines not only led to a reversal of the PARP cleavage impacted by afatinib (Figure 14A), but also resulted in a reduction in the proportion of Annexin V-positive cells as compared to the control (Figure 14B). In addition, the introduction of p-mTOR by MHY1485 was found to restore Mcl-1 protein expression, which had been reduced by afatinib (Figure 14C). On the other hand, the combination of afatinib with rapamycin significantly reduced cell viability and increased cleaved PARP expression and the proportion of Annexin V-positive cells, as compared to treatment with

afatinib alone (Figures 15B, 16A and 16B). Furthermore, the co-treatment of afatinib with rapamycin resulted in a more significant reduction in Mcl-1 expression than treatment of afatinib alone (Figure 16C). These results indicate that mTOR is effectively downregulated by Afatinib and acts as a direct linker that regulates Mcl-1. Therefore, Afatinib induces apoptosis in human oral cancer cells by modulating the EGFR/mTOR/Mcl-1 signaling pathway.

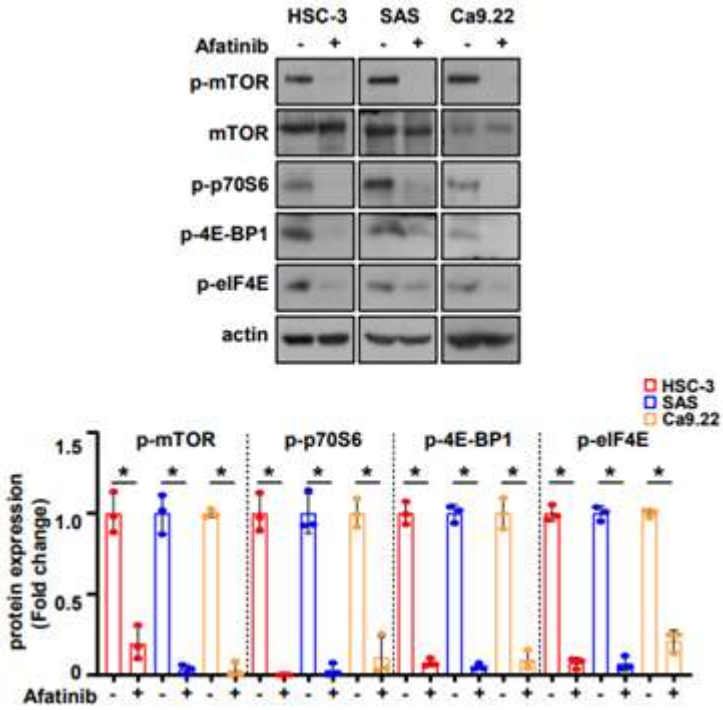

Figure 12. Effects of afatinib on the mTOR signaling pathway in oral cancer cell lines. HSC-3, SAS, and Ca9.22 cells were treated with afatinib (0 and 8 μM) for 24 hours and expression of p-mTOR$^{(Ser2448)}$, p-P70S6K$^{(Thr389)}$, p-4E-BP1$^{(Thr37/46)}$, and p-eIF4E$^{(Ser209)}$ in oral cancer cell lines was determined by Western blot analysis. The graph displays the means ± SD of three independent experiments. *$P < 0.05$ by two-tailed Student's *t*-test.

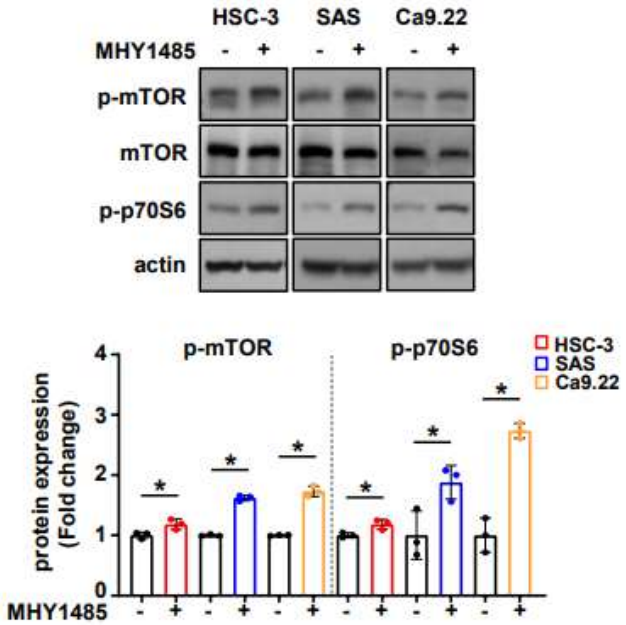

Figure 13. Effects of MHT1485 on the protein expression of p-p70S6$^{(Thr389)}$ in oral cancer cell lines. The cells were treated with DMSO or MHY 1485 (HSC-3 cell line; 0.0625 μM, SAS cell line; 0.125 μM, and Ca9.22 cell line; 0.125 μM) for 25 hours. The expression of p-p70S6$^{(Thr389)}$ in oral cancer cell lines was determined by Western blot analysis. The graph displays the means ± SD of three independent experiments. *$P < 0.05$ by two-tailed Student's *t*-test.

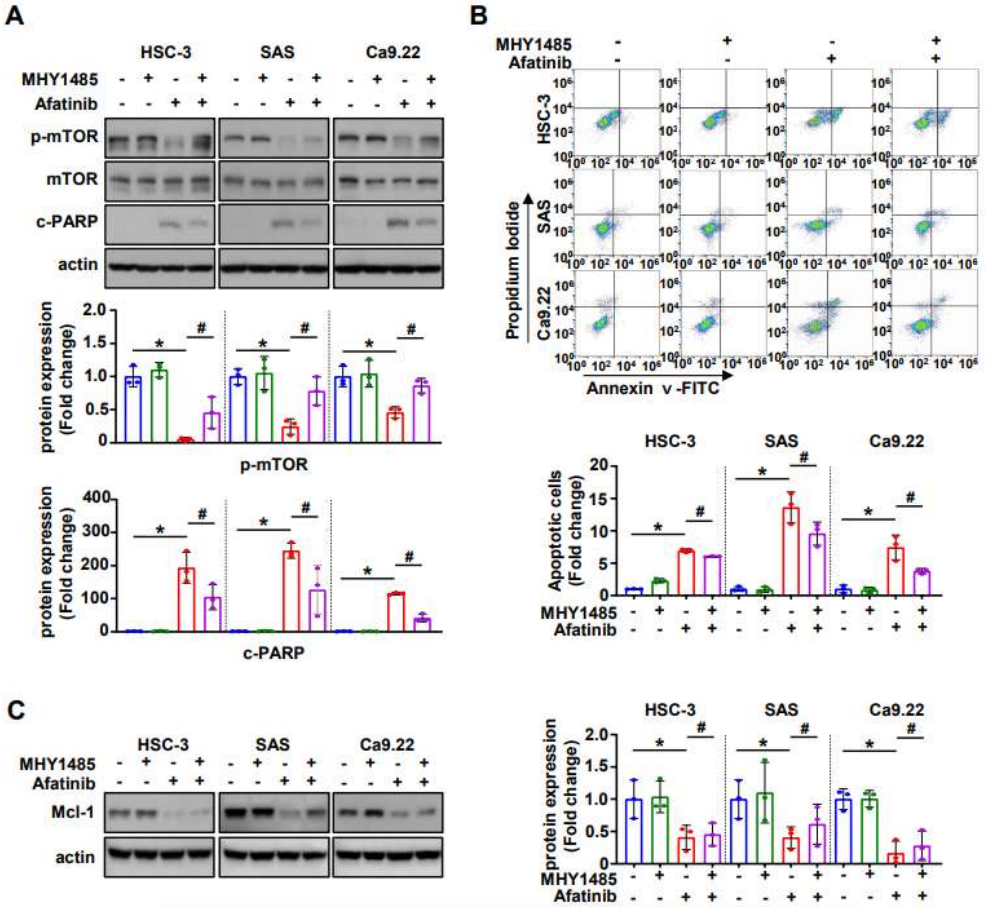

Figure 14. Apoptotic effect of afatinib in oral cancer cell lines is mediated through the depletion of mTOR protein via the EGFR/mTOR/MCL-1 axis. The cells were treated with MHY 1485 (HSC-3 cell line; 0.0625 μM, SAS cell line; 0.125 μM, and Ca9.22 cell line; 0.125 μM) for 1 hour followed by direct treatment with afatinib for 24 hours. (A) p-mTOR and cleaved PARP protein expression levels were assessed by Western blot analysis. (B) To quantify the proportion of apoptotic cells, Annexin V/PI staining was

performed. (C) The expression levels of Mcl-1 protein were evaluated by Western blot analysis. The graph displays the means ± SD of three independent experiments. *$P < 0.05$ by one-way ANOVA.

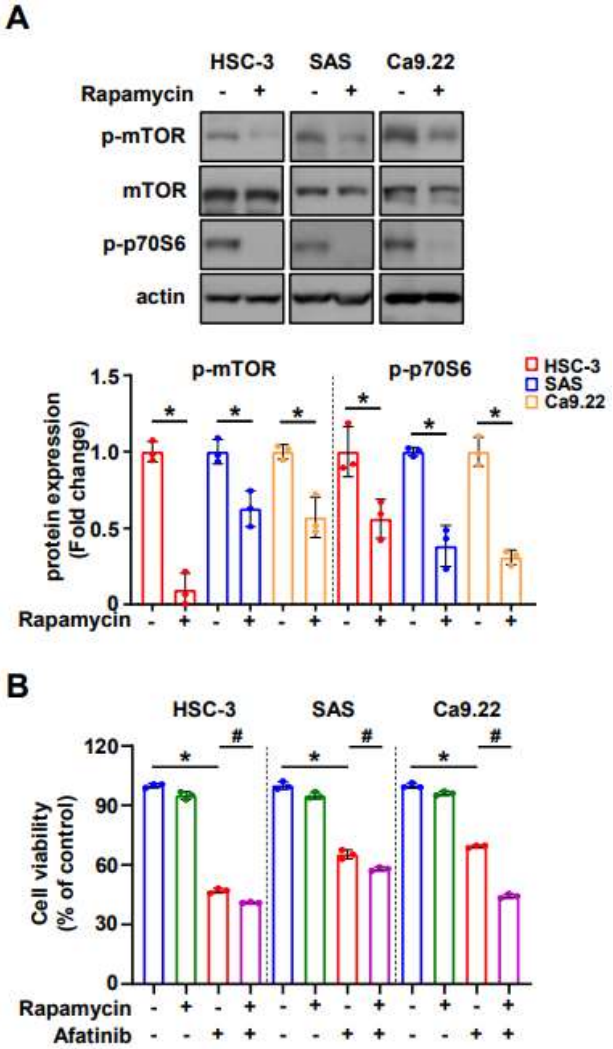

Figure 15. Effects of rapamycin and afatinib on cell viability in oral cancer cell lines (A) HSC-3, SAS, and Ca9.22 cells were treated with DMSO or rapamycin (100 nM) for 25 hours and expression of p-mTOR and p-p70S6 in oral cancer cell lines was determined by Western blot analysis. (B) Cell viability was assessed using a trypan blue exclusion assay. The cells were

treated with rapamycin 100nM for 1 hour followed by direct treatment with afatinib for 24 hours. The graph displays the means ± SD of three independent experiments. *$P < 0.05$ by one-way ANOVA.

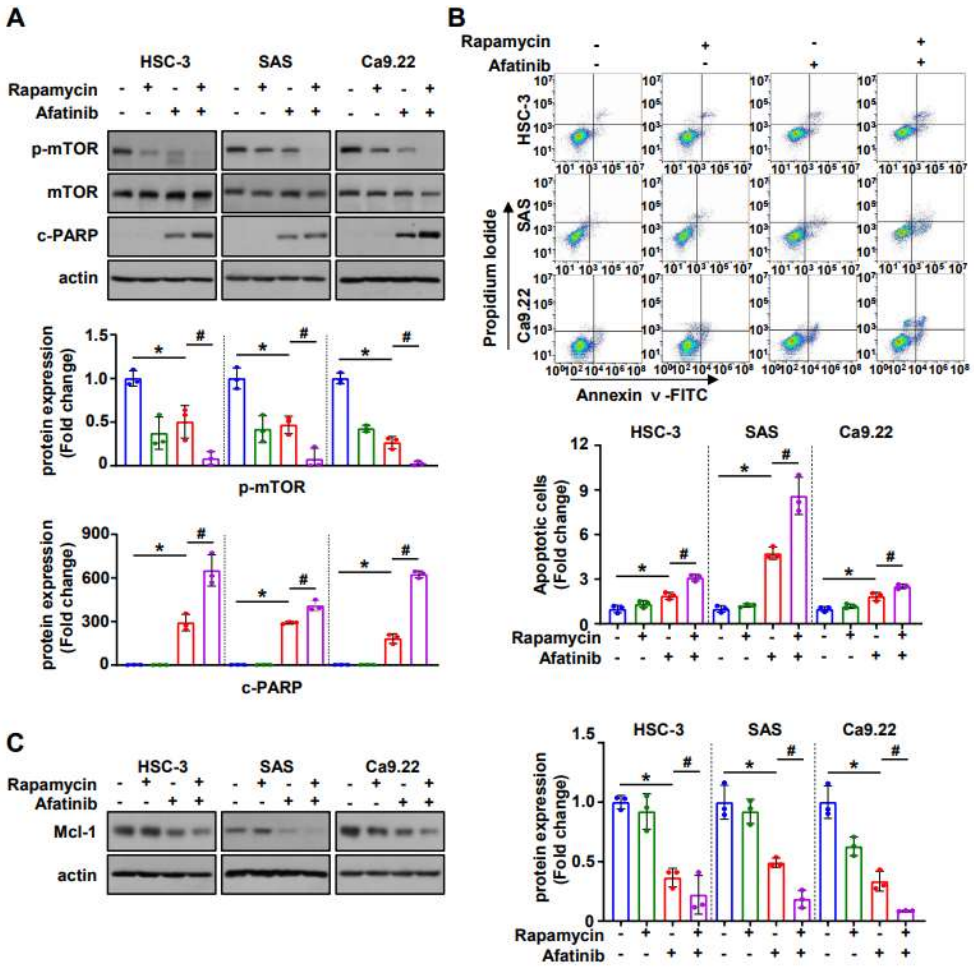

Figure 16. Apoptotic effect of afatinib via the EGFR/mTOR/MCL-1 axis in oral cancer cell lines. The cells were treated with rapamycin 100nM for 1 hour followed by direct treatment with afatinib for 24 hours. (A) p-mTOR, mTOR and c-PARP protein expression levels were assessed by Western blot analysis. (B) To quantify the proportion of apoptotic cells, Annexin V/PI staining was performed. (C) The expression levels of Mcl-1 protein were

evaluated by Western blot analysis. The graph displays the means ± SD of three independent experiments. *$P < 0.05$ by one-way ANOVA.

3.12 Afatinib shows superior anti-cancer activity and Mcl-1 inhibition in oral cancer cell lines compared to gefitinib.

In order to compare the anticancer effects of gefitinib (a first-generation EGFR TKI) and afatinib in human oral cancer cell lines, I treated the three oral cancer cell lines with two EGFR TKIs at equal concentration and for the same duration of time, followed by measuring cell viability. The results showed that afatinib significantly inhibited cell growth compared to gefitinib (Figure 17A). I also found higher expression of c-PARP in all three cell lines when treated with afatinib compared to gefitinib using Western blotting, and detected a higher proportion of Annexin V-positive cells using Annexin V/PI staining (Figures 17B and 17C). Furthermore, it was confirmed that afatinib remarkably downregulated Mcl-1 expression in HSC-3, SAS, and Ca9.22 cell lines compared to gefitinib (Figure 18). All these findings suggest that afatinib exhibits superior anti-cancer activity in oral cancer cell lines compared to gefitinib.

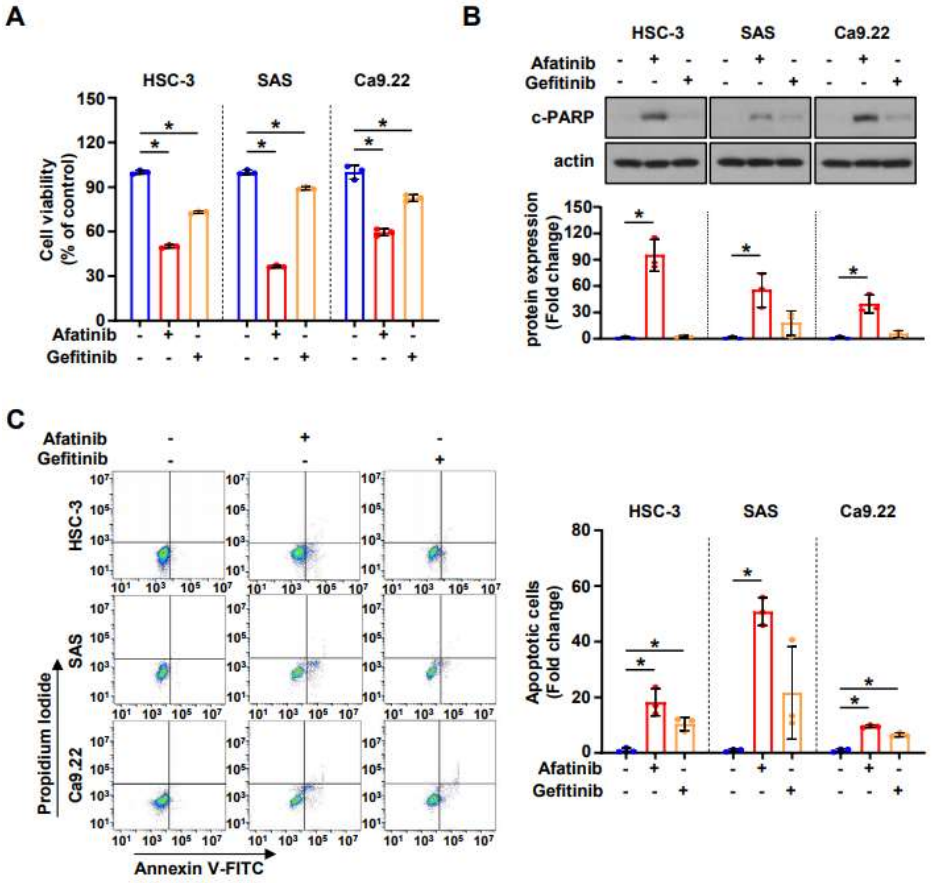

Figure 17. Comparison of the growth inhibitory and apoptosis-inducing effects between afatinib and gefitinib in oral cancer cell lines. HSC-3, SAS, and Ca9.22 cells were treated with DMSO, 8 μM of afatinib, and gefitinib for 24 hours. (A) Cell viability was assessed using a trypan blue exclusion assay. (B) The expression level of c-PARP protein was evaluated by Western blot analysis. (C) To quantify the proportion of apoptotic cells, Annexin V/PI staining was performed. The graph displays the means ± SD of three independent experiments. *P< 0.05 by one-way ANOVA.

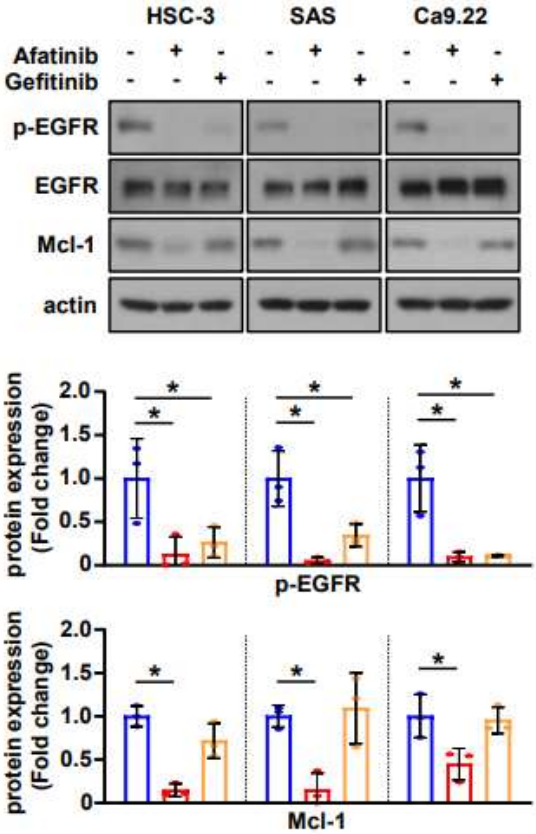

Figure 18. Comparison of p-EGFR and Mcl-1 protein expression reduction between afatinib and gefitinib in oral cancer cell lines. HSC-3, SAS, and Ca9.22 cells were treated with DMSO, 8 μM of afatinib, and gefitinib for 24 hours, and the expression of p-EGFR and Mcl-1 was analyzed by Western blot analysis. The graph displays the means ± SD of three independent experiments. *P< 0.05 by one-way ANOVA.

3.13 Afatinib effectively suppresses tumor growth in a xenograft model with no detectable toxicity.

To assess the *in vivo* antitumor activity of afatinib, I used a xenograft mouse model by transplanting HSC-3 cells into the flank of athymic nude mice. The results of treatment with afatinib showed a statistically significant reduction in tumor volume starting from day 14 after treatment in the group treated with 50mg/kg of afatinib. Moreover, there was an evident dose-dependent trend in tumor size reduction with increasing concentrations of afatinib treatment. (Figures 19A and 19B). In the xenograft mouse model's tumor tissues, IHC staining was conducted to evaluate the efficacy of afatinib in regulating the expression of p-EGFR, Mcl-1, and c-caspase. The results showed that, compared with the control group, treatment with afatinib significantly decreased the expression of p-EGFR and Mcl-1. The expression of c-caspase3 did not show a statistically significant increase; however, there was a trend toward increased protein expression in an afatinib concentration-dependent manner (Figures 19C). To evaluate the in vivo biocompatibility of afatinib, I measured the body weight and the weights of the liver and kidneys. There were no significant changes in body weight or organ weights following treatment with afatinib (Figures 20A and 20B). In addition, histopathologic evaluation of the liver and kidney did not show any pathological differences

between the control- and afatinib-treated mice (Figures 20C). These results demonstrate that afatinib exerts an anti-tumorigenic effect, without any detectable in vivo adverse effects.

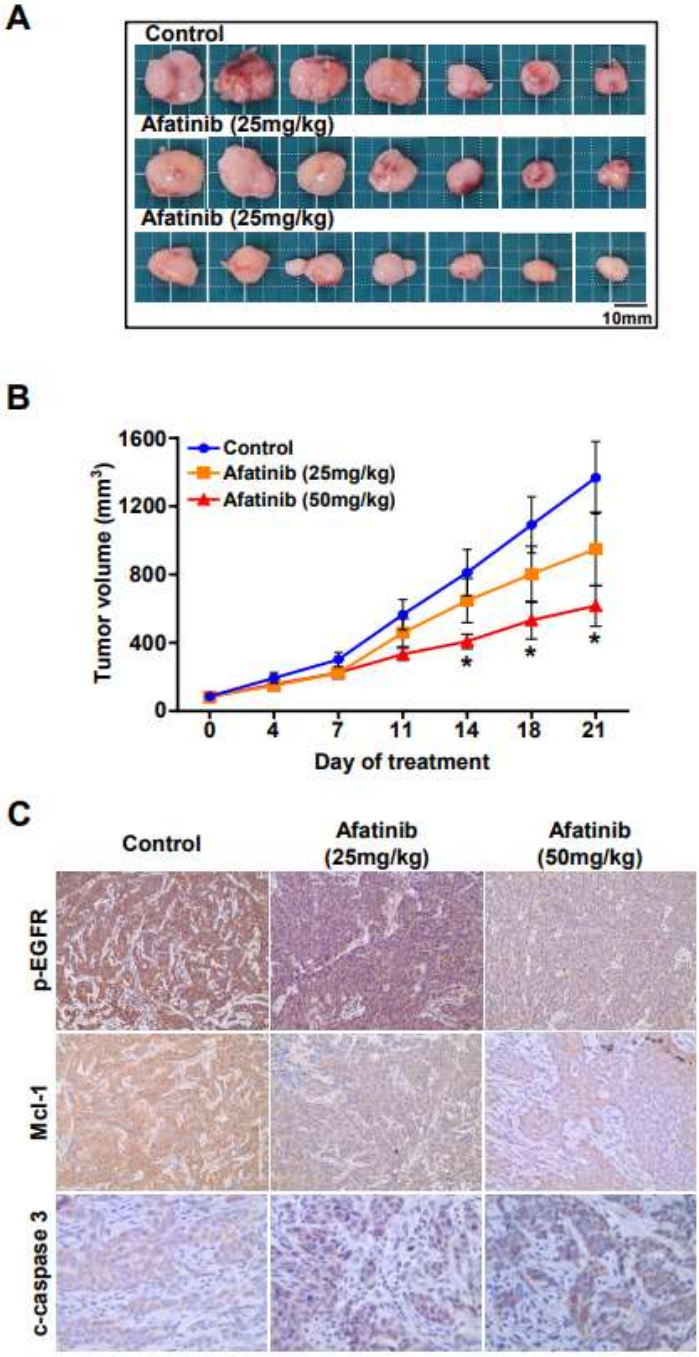
A
Control
Afatinib (25mg/kg)
Afatinib (25mg/kg)
10mm
B
Control
Afatinib (25mg/kg)
Afatinib (50mg/kg)
Tumor volume (mm³)
1600
1200
800
400
0
0
4
7
11
14
18
21
Day of treatment
C
Control
Afatinib (25mg/kg)
Afatinib (50mg/kg)
p-EGFR
Mcl-1
c-caspase 3

Figure 19. Anti-tumor capacity of afatinib *in vivo* against human oral cancer. A vehicle control or 25 mg/kg/day and 50 mg/kg/day of afatinib were orally administered five times per week for 21 days to nude mice implanted with HSC-3 cells. (A) Images of tumor specimens. (B) Tumor volume were measured as described in Materials and methods section. (C) The expression of p-EGFR, Mcl-1, and c-caspase 3 proteins in tumor tissues was evaluated using IHC staining (p-EGFR and Mcl-1: magnification, × 200; c-caspase 3: magnification, × 400).

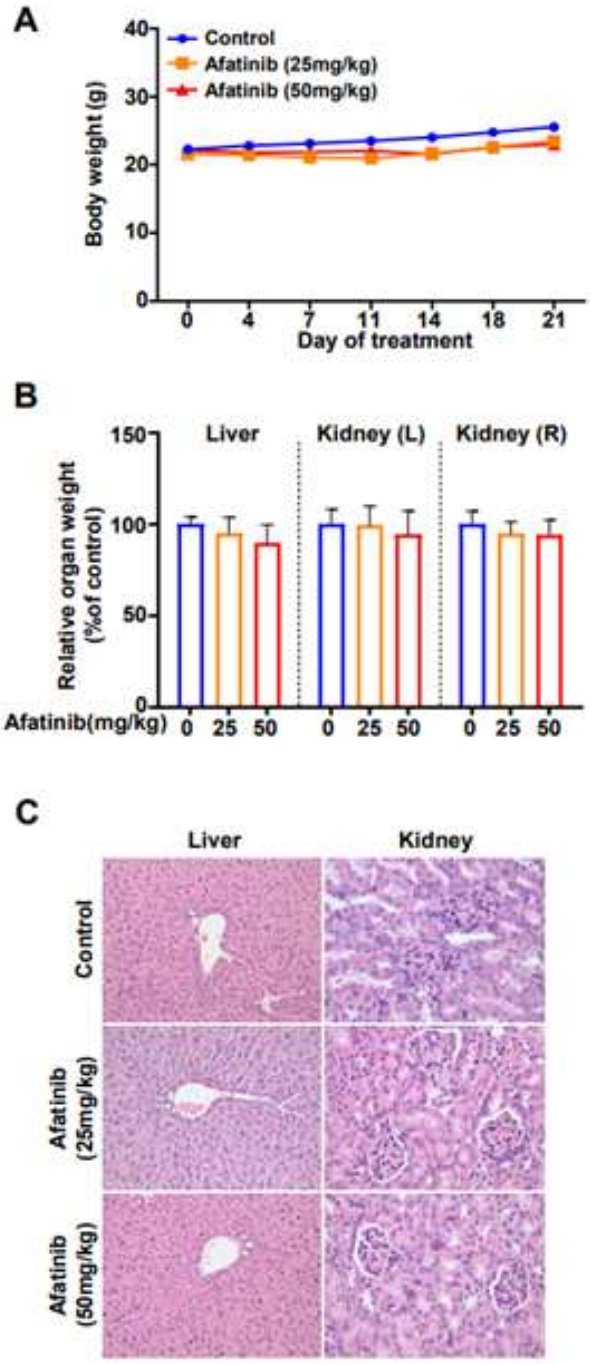
A
Control
Afatinib (25mg/kg)
Afatinib (50mg/kg)
Body weight (g)
40
30
20
10
0
0
4
7
11
14
18
21
Day of treatment
B
Liver
Kidney (L)
Kidney (R)
Relative organ weight (%of control)
150
100
50
0
Afatinib(mg/kg)
0
25
50
C
Liver
Kidney
Control
Afatinib (25mg/kg)
Afatinib (50mg/kg)

Figure 20. Evaluation of the side effects of afatinib *in vivo* against human oral cancer. (A) Body weight were measured as described in Materials and methods section. (B) Liver and kidney were surgically excised and their respective weights were measured. The graph displays the means ± SD. *P< 0.05 by Mann-Whitney test in SPSS. (C) Histopathological alterations of liver and kidney were visualized by H&E staining (liver: magnification, × 200; kidney: magnification, × 400).

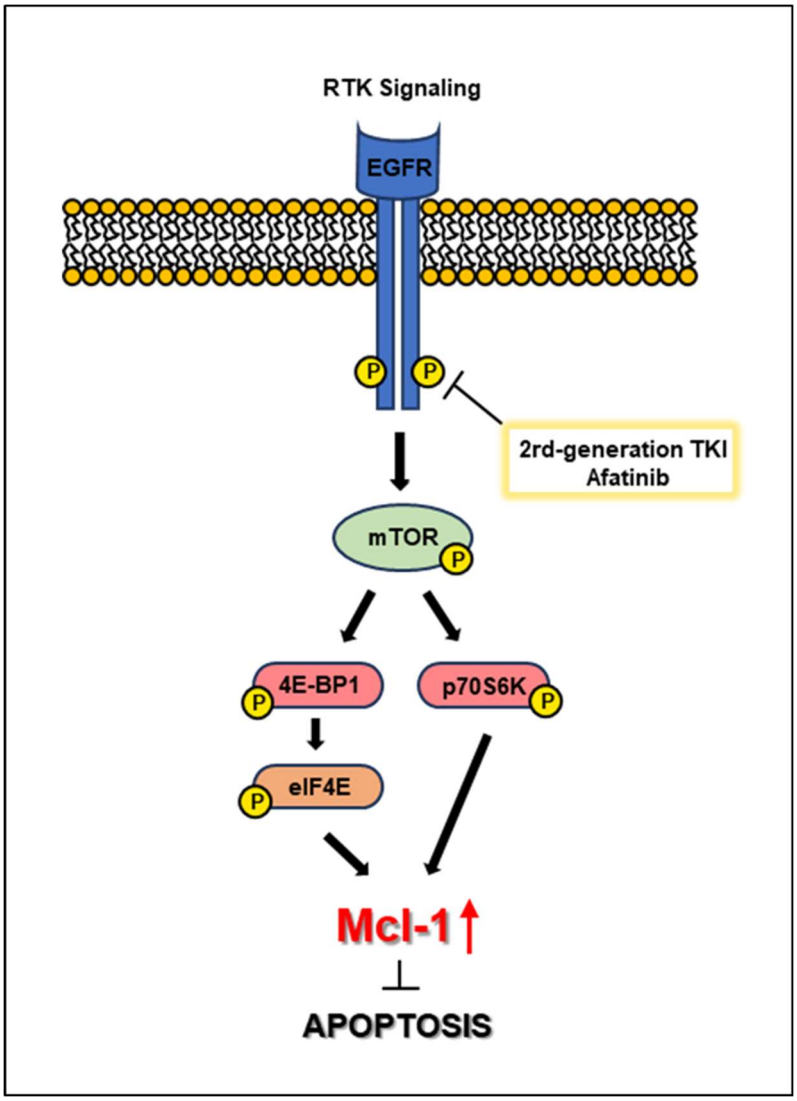

Figure 21. Graphical figure. In oral cancer, afatinib effectively inhibits the activation of mTOR, a downstream signaling of EGFR, thereby regulating the expression of translational factors and ultimately suppressing the expression of Mcl-1, leading to cell apoptosis. This demonstrates the potential of afatinib as an effective anticancer agent in oral cancer.

4. Discussion

Although previous studies have reported the anti-cancer effects of afatinib in various human cancers, there is a lack of research that elucidates the molecular and biological mechanisms of afatinib's anti-cancer efficacy in oral cancer. In this study, the apoptotic activity of afatinib against human oral cancer was measured *in vitro* and *in vivo* to evaluate its potential as an anti-cancer drug candidate.

Programmed cell death, also known as apoptosis, is precisely controlled at the genetic level, allowing for the organized and efficient elimination of damaged cells, such as those that result from DNA damage or during tissue development [36]. The process of apoptosis plays a crucial role in a number of physiological processes, including tissue development and the immune response. As such, the proper regulation of apoptosis is essential for maintaining tissue homeostasis. However, deregulation of apoptosis can contribute to a range of pathological conditions, such as carcinogenesis and chemotherapy resistance [37]. The process of apoptosis is mainly regulated by the activation or inhibition of caspases, which are enzymes responsible for the degradation of various substrates within the cell. This leads to a range of biochemical and morphological alterations, including mitochondrial outer membrane permeabilization, cell membrane remodeling and blebbing, cell

shrinkage, nuclear condensation, and DNA fragmentation, ultimately resulting in programmed cell death [38]. In this study, I confirmed the cell growth-inhibitory and apoptosis-inducing effects of afatinib in oral cancer cell lines. Furthermore, the expression of Mcl-1 was downregulated without any changes in mRNA levels (Figure 7, 8). Recent studies have reported that EGFR and Mcl-1 play important roles in the proliferation and survival of various types of cancer, and that afatinib is a drug that induces apoptosis by regulating EGFR and Mcl-1 [39]. In this paper, I confirmed through *in silico* analysis that both EGFR and Mcl-1 are highly expressed in HNC and are crucial factors associated with poor prognosis in patients (Figure 1, 2). In addition, I analyzed for the first time the correlation between Mcl-1 and EGFR expression in oral cancer. *In silico* analysis showed a positive correlation between EGFR and Mcl-1 mRNA expression, indicating that the concurrent high expression of these two factors plays a crucial role in poor prognosis in patients compared to when they are not both highly expressed (Figure 3). Furthermore, as seen in Figures 4 and 5, I also confirmed a high correlation between the expression of these two factors in oral cancer patient tissues and human oral cancer cell lines. These findings suggest that devising therapeutic strategies targeting both EGFR and Mcl-1 could serve as an effective approach for the treatment of oral cancer patients. Therefore, I

investigated whether the regulation of Mcl-1 expression could be effectively controlled by treating oral cancer cell lines with afatinib, which modulates EGFR expression, and aimed to explore the associated signaling mechanisms.

In the intrinsic pathway of apoptosis involving Mcl-1, several key components contribute to the regulation and execution of this complex process [40]. Mcl-1, an anti-apoptotic member of the Bcl-2 family, plays a pivotal role in controlling mitochondrial outer membrane permeabilization (MOMP), a critical step in initiating apoptosis [41]. During MOMP, the mitochondrial outer membrane becomes permeable, leading to the release of cytochrome c from the mitochondrial intermembrane space into the cytosol. Once in the cytosol, cytochrome c associates with apoptotic protease activating factor-1 (Apaf-1) and pro-caspase-9, forming a multi-protein complex called the apoptosome. The apoptosome activates caspase-9, which in turn activates downstream effector caspases, such as caspase-3, leading to the execution of apoptosis [42, 43]. Mcl-1 interacts with various pro-apoptotic proteins, including Bim and t-Bid, to regulate apoptosis. Bim, a BH3-only protein, can bind to Mcl-1, neutralizing its anti-apoptotic function and thus promoting apoptosis. Bim is capable of activating pro-apoptotic Bcl-2 family members Bax and Bak, which oligomerize and form pores in the mitochondrial outer membrane, facilitating MOMP. Conversely, t-Bid, a

truncated form of the pro-apoptotic protein Bid, can also trigger MOMP by activating Bax and Bak. t-Bid is generated by the cleavage of Bid by active caspase-8, which is initiated in the extrinsic pathway of apoptosis. Once activated, t-Bid translocates to the mitochondria, where it interacts with Mcl-1 and other Bcl-2 family members to modulate MOMP [44, 45]. The mitochondrial membrane potential (MMP) was measured using the JC-1 assay, confirming the functional changes induced by afatinib in oral cancer cell lines. Moreover, the release of cytochrome c into the cytoplasm was observed, indicating the activation of mitochondrial-mediated intrinsic apoptosis. According to the results, it was found that afatinib induces intrinsic apoptosis via the mitochondrial pathway (Figure 11). I observed an increase in the expression of Bim, a protein known to bind to the mitochondrial membrane, causing damage and inducing the release of cytochrome c. Bim also interacts with Mcl-1 to regulate cell survival and apoptosis[46]. Specifically, the results of this study showed a significant increase in the expression of the Bim_{EL} isoform of Bim in all three cell lines (Figure 10). Bim_{EL}, the longest isoform among Bim proteins, plays a crucial role in the sensitivity to anti-cancer drugs and the regulation of cell death. In a previous study, it was reported that Bim_{EL} interacts with Mcl-1 to inhibit its function and induce apoptosis in tumor cells, thereby overcoming Mcl-1-mediated

resistance to apoptosis [47]. In this study, I aimed to ascertain if afatinib-induced apoptosis in oral cancer cell lines was mediated by Mcl-1. To carry out the experiments, an Mcl-1 over-expression vector and a transient transfection system were utilized. In HSC-3, SAS, and Ca9.22 cell lines, Mcl-1 overexpression significantly restored cell viability and counteracted the cleavage of PARP previously affected by afatinib. Moreover, I noticed a decrease in apoptotic effects in cells with Mcl-1 overexpression compared to the control group, validating the presence of Mcl-1 mediated cell death. In summary, our results highlight the importance of Mcl-1 as a key target in afatinib-induced apoptosis in oral cancer cell lines (Figure 9).

The mammalian target of rapamycin (mTOR) signaling pathway serves as a key hub connecting multiple signaling pathways, and its regulation is mediated in part by the upstream protein EGFR. Upon activation, EGFR initiates a cascade of reactions. Initially, the regulatory subunits of PI3K, p85, undergo dimerization and release its catalytic subunit p110. p110 then facilitates the phosphorylation of the membrane protein phosphatidylinositol-(3,4)-bisphosphate (PIP2), converting it into phosphatidylinositol-(3,4,5)-trisphosphate (PIP3). PIP3 subsequently recruits Akt, a downstream effector, to the inner membranes and enables its phosphorylation at the serine/threonine kinase sites (Thr308 and Ser473) by phosphoinositide-

dependent kinase 1/2 (PDK1/2). Activated Akt plays a crucial role in the downstream response mediated by mTOR, which involves protein and ribosome biogenesis [48]. In preclinical studies conducted abroad, combination therapy with inhibitors targeting both EGFR and the mTOR pathway has been investigated [49]. Based on previous studies, the mTOR signaling pathway has been reported to promote cancer growth by enhancing the stability and expression of Mcl-1 protein. In light of these findings, I aimed to investigate whether mTOR may serve as a direct linker between EGFR and Mcl-1 [50]. The mTOR pathway operates through two distinct protein complexes, known as mTOR complex 1 (mTORC1) and mTOR complex 2 (mTORC2). mTORC1 consists of mTOR, mLST8, Raptor, and PRAS40, and is responsible for activating the p70S6K, while simultaneously inhibiting 4E-BP1. This, in turn, leads to an increase in protein synthesis and cellular growth. On the other hand, mTORC2 is composed of mTOR, Sin1, Rictor, and mLST8, and plays a crucial role in the activation of Akt. By phosphorylating and activating Akt, mTORC2 promotes cell survival and proliferation [51]. The protein kinase p70S6K plays a crucial role in cell growth and G1 cell cycle progression, and is activated as part of a signaling pathway that involves mTOR. Multiple phosphorylation events within the catalytic, linker, and pseudosubstrate domains of p70S6K control its activity,

ultimately leading to the specific phosphorylation of ribosomal protein S6. Among these phosphorylation events, activation of p70S6K occurs via phosphorylation at ser411, Thr421, and Ser424 within the pseudosubstrate region, while phosphorylation of Thr229 in the catalytic domain and Thr389 in the linker domain are most critical for kinase function [52]. Many recent studies have focused on the interaction between the mTOR pathway and Mcl-1, and how this interaction affects chemoresistance. Mcl-1 is one of the cell survival factors that can contribute to chemoresistance. Combination therapy with mTOR inhibitors has shown the potential to overcome chemoresistance by suppressing the survival signals mediated by Mcl-1. These findings demonstrate that targeting Mcl-1 through mTOR inhibition may represent a promising strategy for overcoming chemoresistance in various cancers. In this study, I confirmed that the activity of mTOR is inhibited by afatinib and investigated whether the mTOR pathway is involved in the regulation of Mcl-1 expression. As a result of verifying whether afatinib regulates the mTOR signaling pathway, the expression of p-P70S6K$^{(Thr389)}$, p-4E-BP1$^{(Thr37/46)}$, and p-eIF4E$^{(Ser209)}$ was effectively reduced. Further experiments were performed using an mTOR inhibitor and activator to determine whether the expression of Mcl-1, which is regulated by afatinib, is mTOR-dependent. The expression of c-PARP, induced by afatinib, was reduced by treatment with an mTOR

activator, and a decrease in the apoptotic cell ratio was confirmed along with turnover of Mcl-1 expression. Similar results were observed when treated with an mTOR inhibitor (Figure 12-16). These results indicate that afatinib post-transcriptionally regulates the expression of Mcl-1 protein in an mTOR-dependent manner in oral cancer cell lines. Taken together, the findings suggest that dual regulation of mTOR and Mcl-1 may represent a highly effective therapeutic strategy for cancer treatment. By targeting both pathways simultaneously, it may be possible to overcome chemoresistance and improve overall treatment efficacy in a range of cancers. These results provide strong support for the continued development of novel combination therapies targeting both mTOR and Mcl-1 as a promising approach to cancer treatment.

Previous studies have reported that in T790M-positive non-small cell lung cancer (NSCLC) patients who have failed initial EGFR-TKI treatment, the third-generation EGFR tyrosine kinase inhibitor osimertinib exhibits superior antitumor efficacy compared to afatinib by specifically targeting the T790M mutation. In the present study, oral cancer cell lines were utilized for research purposes, and since the presence of the T790M mutation was not detected in these cell lines (Figure 6), it was deemed appropriate to conduct research focusing on pre-third-generation EGFR tyrosine kinase inhibitors [53]. There

are inherent differences in the mechanism of action between first-generation EGFR tyrosine kinase inhibitors, such as gefitinib and erlotinib, and the second-generation ErbB family blocker, afatinib. The first-generation inhibitors reversibly bind to and inhibit EGFR signaling, while afatinib irreversibly blocks signaling from all relevant homo- and hetero-dimers of the ErbB family receptors. This broader spectrum of activity and irreversible mechanism of action of afatinib is believed to contribute to its improved inhibition of EGFR-dependent tumor growth compared to the first-generation EGFR tyrosine kinase inhibitors [54]. Therefore, I compared the anti-tumor efficacy of afatinib and gefitinib in oral cancer cell lines. As shown in Figure 17, afatinib effectively inhibited cell proliferation and exhibited superior apoptotic efficacy compared to gefitinib. Furthermore, it significantly suppressed the expression of Mcl-1 compared to gefitinib (Figure 18).

Multiple studies have demonstrated that the administration of afatinib effectively suppressed tumor growth in live organisms without causing any toxicity or inducing weight loss [55, 56]. Nevertheless, there have been no studies conducted using animal models to investigate the effects of afatinib on human oral cancer. In the present study, it was observed that the administration of afatinib successfully suppressed tumor growth without inducing any weight loss or histopathological changes in the liver and kidney

tissues (Figure 19, 20). These results further reinforce the existing body of research on the efficacy of afatinib.

The development of therapies targeting ErbB receptors has revolutionized the treatment of various malignant diseases. However, many patients experience cancer relapse due to resistance to treatment and metastasis. To overcome this challenge, there is a growing recognition of the need to develop novel ErbB-based combination therapies to delay resistance and maximize treatment efficacy. Afatinib has a low potential for drug-drug interactions, making it a suitable partner for combination therapy with various other anti-cancer agents. There is preclinical rationale for combining afatinib with inhibitors targeting other intracellular signaling pathways, including PI3K/Akt/mTOR, SRC kinase, Ras/Raf/MEK/ERK, and JAK/STAT. Additionally, it can be combined with inhibitors targeting other growth factor receptors such as VEGFR and IGF-1R, other ErbB inhibitors, and immune checkpoint inhibitors. Several early-phase clinical trials are currently ongoing or planned to investigate these combination therapies [57]. There is a need for further research in investigating the efficacy of afatinib as a single agent in oral cancer, and beyond that, exploring novel afatinib-based combination therapies to effectively sustain its anticancer effects.

Although in-depth molecular and biological studies on the mechanisms underlying the anti-cancer effects of afatinib in a tumor xenograft mouse model are still needed, overall, this study has sufficiently demonstrated the induction of cell apoptosis through the regulation of the EGFR/mTOR/Mcl-1 signaling pathway by afatinib in oral cancer. These findings suggest the potential of afatinib as a targeted anti-cancer agent for the treatment of oral cancer (Figure 21).

References

1. Levantini, E., et al., *EGFR signaling pathway as therapeutic target in human cancers.* Semin Cancer Biol, 2022. **85**: p. 253-275.
2. Rajaram, P., et al., *Epidermal growth factor receptor: Role in human cancer.* Indian J Dent Res, 2017. **28**(6): p. 687-694.
3. Ayati, A., et al., *A review on progression of epidermal growth factor receptor (EGFR) inhibitors as an efficient approach in cancer targeted therapy.* Bioorg Chem, 2020. **99**: p. 103811.
4. Lv, X.X., et al., *EGFR enhances the stemness and progression of oral cancer through inhibiting autophagic degradation of SOX2.* Cancer Med, 2020. **9**(3): p. 1131-1140.
5. Maemondo, M., et al., *Gefitinib or chemotherapy for non-small-cell lung cancer with mutated EGFR.* N Engl J Med, 2010. **362**(25): p. 2380-8.
6. Chitturi, K.R., et al., *Cardiovascular Risks with Epidermal Growth Factor Receptor (EGFR) Tyrosine Kinase Inhibitors and Monoclonal Antibody Therapy.* Curr Oncol Rep, 2022. **24**(4): p. 475-491.
7. Adams, G.P. and L.M. Weiner, *Monoclonal antibody therapy of cancer.* Nat Biotechnol, 2005. **23**(9): p. 1147-57.
8. Singh, M. and H.R. Jadhav, *Targeting non-small cell lung cancer with small-molecule EGFR tyrosine kinase inhibitors.* Drug Discov Today, 2018. **23**(3): p. 745-753.
9. Nguyen, K.S., S. Kobayashi, and D.B. Costa, *Acquired resistance to epidermal growth factor receptor tyrosine kinase inhibitors in non-small-cell lung cancers dependent on the epidermal growth factor receptor pathway.* Clin Lung Cancer, 2009. **10**(4): p. 281-9.
10. Solca, F., et al., *Target binding properties and cellular activity of afatinib (BIBW 2992), an irreversible ErbB family blocker.* J Pharmacol Exp Ther, 2012. **343**(2): p. 342-50.
11. Katakami, N., et al., *LUX-Lung 4: a phase II trial of afatinib in patients with advanced non-small-cell lung cancer who progressed during prior treatment with erlotinib, gefitinib, or both.* J Clin Oncol, 2013. **31**(27): p.

3335-41.

12. Schuler, M., et al., *Afatinib beyond progression in patients with non-small-cell lung cancer following chemotherapy, erlotinib/gefitinib and afatinib: phase III randomized LUX-Lung 5 trial.* Ann Oncol, 2016. **27**(3): p. 417-23.
13. Wu, S.G., et al., *The mechanism of acquired resistance to irreversible EGFR tyrosine kinase inhibitor-afatinib in lung adenocarcinoma patients.* Oncotarget, 2016. **7**(11): p. 12404-13.
14. Kishikawa, T., et al., *Osimertinib, a third-generation EGFR tyrosine kinase inhibitor: A retrospective multicenter study of its real-world efficacy and safety in advanced/recurrent non-small cell lung carcinoma.* Thorac Cancer, 2020. **11**(4): p. 935-942.
15. Siegel, R.L., K.D. Miller, and A. Jemal, *Cancer statistics, 2020.* CA Cancer J Clin, 2020. **70**(1): p. 7-30.
16. Hassanein, K.A., B.T. Musgrove, and E. Bradbury, *Functional status of patients with oral cancer and its relation to style of coping, social support and psychological status.* Br J Oral Maxillofac Surg, 2001. **39**(5): p. 340-5.
17. Cheng, Y., et al., *The Molecular Basis and Therapeutic Aspects of Cisplatin Resistance in Oral Squamous Cell Carcinoma.* Front Oncol, 2021. **11**: p. 761379.
18. Sigismund, S., D. Avanzato, and L. Lanzetti, *Emerging functions of the EGFR in cancer.* Mol Oncol, 2018. **12**(1): p. 3-20.
19. Yewale, C., et al., *Epidermal growth factor receptor targeting in cancer: a review of trends and strategies.* Biomaterials, 2013. **34**(34): p. 8690-707.
20. Dong, R.F., et al., *EGFR mutation mediates resistance to EGFR tyrosine kinase inhibitors in NSCLC: From molecular mechanisms to clinical research.* Pharmacol Res, 2021. **167**: p. 105583.
21. Zandi, R., et al., *Mechanisms for oncogenic activation of the epidermal growth factor receptor.* Cell Signal, 2007. **19**(10): p. 2013-23.
22. Vokes, E.E. and E. Chu, *Anti-EGFR therapies: clinical experience in colorectal, lung, and head and neck cancers.* Oncology (Williston Park), 2006. **20**(5 Suppl 2): p. 15-25.

23. Cohen, R.B., *Current challenges and clinical investigations of epidermal growth factor receptor (EGFR)- and ErbB family-targeted agents in the treatment of head and neck squamous cell carcinoma (HNSCC).* Cancer Treat Rev, 2014. **40**(4): p. 567-77.
24. Yun, C.H., et al., *The T790M mutation in EGFR kinase causes drug resistance by increasing the affinity for ATP.* Proc Natl Acad Sci U S A, 2008. **105**(6): p. 2070-5.
25. Takezawa, K., et al., *HER2 amplification: a potential mechanism of acquired resistance to EGFR inhibition in EGFR-mutant lung cancers that lack the second-site EGFRT790M mutation.* Cancer Discov, 2012. **2**(10): p. 922-33.
26. Oxnard, G.R., et al., *New strategies in overcoming acquired resistance to epidermal growth factor receptor tyrosine kinase inhibitors in lung cancer.* Clin Cancer Res, 2011. **17**(17): p. 5530-7.
27. Wecker, H. and C.F. Waller, *Afatinib.* Recent Results Cancer Res, 2018. **211**: p. 199-215.
28. Jain, P., et al., *Afatinib and lung cancer.* Expert Rev Anticancer Ther, 2014. **14**(12): p. 1391-406.
29. Craig, R.W., *MCL1 provides a window on the role of the BCL2 family in cell proliferation, differentiation and tumorigenesis.* Leukemia, 2002. **16**(4): p. 444-54.
30. Warr, M.R. and G.C. Shore, *Unique biology of Mcl-1: therapeutic opportunities in cancer.* Curr Mol Med, 2008. **8**(2): p. 138-47.
31. Nalluri, S., et al., *EGFR signaling defines Mcl(-)1 survival dependency in neuroblastoma.* Cancer Biol Ther, 2015. **16**(2): p. 276-86.
32. Placzek, W.J., et al., *A survey of the anti-apoptotic Bcl-2 subfamily expression in cancer types provides a platform to predict the efficacy of Bcl-2 antagonists in cancer therapy.* Cell Death Dis, 2010. **1**(5): p. e40.
33. Li, X.X., et al., *Increased MCL-1 expression predicts poor prognosis and disease recurrence in acute myeloid leukemia.* Onco Targets Ther, 2019. **12**: p. 3295-3304.
34. Yu, X., et al., *Formononetin inhibits tumor growth by suppression of EGFR-*

Akt-Mcl-1 axis in non-small cell lung cancer. J Exp Clin Cancer Res, 2020. **39**(1): p. 62.

35. Shi, P., et al., *Overcoming Acquired Resistance to AZD9291, A Third-Generation EGFR Inhibitor, through Modulation of MEK/ERK-Dependent Bim and Mcl-1 Degradation.* Clin Cancer Res, 2017. **23**(21): p. 6567-6579.
36. Fuchs, Y. and H. Steller, *Programmed cell death in animal development and disease.* Cell, 2011. **147**(4): p. 742-58.
37. Pistritto, G., et al., *Apoptosis as anticancer mechanism: function and dysfunction of its modulators and targeted therapeutic strategies.* Aging (Albany NY), 2016. **8**(4): p. 603-19.
38. Dabrowska, C., M. Li, and Y. Fan, *Apoptotic Caspases in Promoting Cancer: Implications from Their Roles in Development and Tissue Homeostasis.* Adv Exp Med Biol, 2016. **930**: p. 89-112.
39. Liu, X., et al., *Afatinib down-regulates MCL-1 expression through the PERK-eIF2alpha-ATF4 axis and leads to apoptosis in head and neck squamous cell carcinoma.* Am J Cancer Res, 2016. **6**(8): p. 1708-19.
40. Wang, H., et al., *Targeting MCL-1 in cancer: current status and perspectives.* J Hematol Oncol, 2021. **14**(1): p. 67.
41. Fletcher, L., et al., *Cell Death Pathways in Lymphoid Malignancies.* Curr Oncol Rep, 2020. **22**(1): p. 10.
42. Wu, C.C. and S.B. Bratton, *Regulation of the intrinsic apoptosis pathway by reactive oxygen species.* Antioxid Redox Signal, 2013. **19**(6): p. 546-58.
43. Gupta, S., et al., *The mitochondrial death pathway: a promising therapeutic target in diseases.* J Cell Mol Med, 2009. **13**(6): p. 1004-33.
44. Hassan, M., et al., *Apoptosis and molecular targeting therapy in cancer.* Biomed Res Int, 2014. **2014**: p. 150845.
45. Yu, H.J., et al., *Inhibition of myeloid cell leukemia-1: Association with sorafenib-induced apoptosis in human mucoepidermoid carcinoma cells and tumor xenograft.* Head Neck, 2015. **37**(9): p. 1326-35.
46. Gong, Y., et al., *Induction of BIM is essential for apoptosis triggered by EGFR kinase inhibitors in mutant EGFR-dependent lung adenocarcinomas.*

PLoS Med, 2007. **4**(10): p. e294.

47. Gillespie, S., et al., *Bim plays a crucial role in synergistic induction of apoptosis by the histone deacetylase inhibitor SBHA and TRAIL in melanoma cells.* Apoptosis, 2006. **11**(12): p. 2251-65.
48. Li, X., et al., *PI3K/Akt/mTOR signaling pathway and targeted therapy for glioblastoma.* Oncotarget, 2016. **7**(22): p. 33440-50.
49. Ma, J., et al., *Dual Target of EGFR and mTOR Suppresses Triple-Negative Breast Cancer Cell Growth by Regulating the Phosphorylation of mTOR Downstream Proteins.* Breast Cancer (Dove Med Press), 2023. **15**: p. 11-24.
50. Mills, J.R., et al., *mTORC1 promotes survival through translational control of Mcl-1.* Proc Natl Acad Sci U S A, 2008. **105**(31): p. 10853-8.
51. Zou, Z., et al., *mTOR signaling pathway and mTOR inhibitors in cancer: progress and challenges.* Cell Biosci, 2020. **10**: p. 31.
52. Artemenko, M., et al., *p70 S6 kinase as a therapeutic target in cancers: More than just an mTOR effector.* Cancer Lett, 2022. **535**: p. 215593.
53. Yang, Y., et al., *Osimertinib versus afatinib in patients with T790M-positive, non-small-cell lung cancer and multiple central nervous system metastases after failure of initial EGFR-TKI treatment.* BMC Pulm Med, 2021. **21**(1): p. 172.
54. Park, K., et al., *Afatinib versus gefitinib as first-line treatment of patients with EGFR mutation-positive non-small-cell lung cancer (LUX-Lung 7): a phase 2B, open-label, randomised controlled trial.* Lancet Oncol, 2016. **17**(5): p. 577-89.
55. Xie, C., et al., *Apatinib triggers autophagic and apoptotic cell death via VEGFR2/STAT3/PD-L1 and ROS/Nrf2/p62 signaling in lung cancer.* J Exp Clin Cancer Res, 2021. **40**(1): p. 266.
56. Feng, H., et al., *Apatinib-induced protective autophagy and apoptosis through the AKT-mTOR pathway in anaplastic thyroid cancer.* Cell Death Dis, 2018. **9**(10): p. 1030.
57. Bennouna, J. and S.R. Moreno Vera, *Afatinib-based combination regimens*

for the treatment of solid tumors: rationale, emerging strategies and recent progress. Future Oncol, 2016. **12**(3): p. 355-72.

국문초록

구강암에서 EGFR 저해제인 Afatinib의 항암 효능 및 새로운 분자기작에 관한 연구

한 정 민

서울대학교 대학원

치의과학과 구강병리학 전공

지도교수: 조 성 대

목적: 아파티닙은 ErbB family 단백질의 티로신 키나아제에 불가역적으로 작용함으로써 여러 암종에서 항암 효과를 나타내는 것으로 알려져 있다. 그러나 구강암에서 아파티닙의 항암 작용 및 분자적 기전에 대한 연구는 미미한 실정이다. 이에 본 연구에서는 구강암에 대한 아파티닙의 세포사멸 효과와 주요 분자 메커니즘을 규명하고자 하였다.

방법: 유전체 데이터베이스인 CCLE, TCGA, GEO, 그리고 CPTAC를 이용한 *in silico* 분석 및 면역조직화학염색을 통해 EGFR과 Mcl-1의 발현 패턴과 구강암에서의 상관관계 및 환자의 예후와의 연관성에 대해 조사하였다. 아파티닙의 항암 효과와 분자적 메커니즘을 연구하기 위해 trypan blue exclusion assay, western blotting analysis, DAPI 염색, flow cytometric analysis, qPCR, 미토콘드리아 막 전위 분석, 과발현 벡터 구축 및 transient transfection system을 이용하였고, 구강암 세포주를 이식한 tumor xenograft model을 통한 *in vivo* 실험을 진행하였다.

결과: *In silico* 분석 및 면역조직화학 염색을 통해, EGFR과 Mcl-1의 발현 수준이 HNC 환자에서 정상 조직에 비해 높았으며, EGFR과 Mcl-1의 고발현이 HNC 환자에서 불량한 예후와 강하게 연관되어 있음이 확인되었다. EGFR 억제제인 아파티닙은 두 단백질의 발현 및 상관 관계가 높은 것으로 나타난 HSC-3, SAS, 그리고 Ca9.22 세포주에서 세포 생존 능력을 억제하고 세포 사멸을 유도하였다. 아파티닙은 mRNA 발현의 변화 없이 Mcl-1 단백질 발현을 효과적으로 하향 조절하였다. transient transfection

system을 사용한 Mcl-1 과발현은 아파티닙이 세포주에 미치는 항증식 및 사멸 촉진 효과를 감소시켰다. 아파티닙은 Mcl-1의 하위 표적인 Bim_{EL} 발현을 상당히 증가시켰으며, 이로 인해 MOMP가 감소하고, cytochrome c가 세포질로 방출되었다. 아파티닙은 또한 구강암 세포주에서 mTOR 신호 전달 경로의 활성화를 감소시켰다. MHY1485, 라파마이신을 사용하여 아파티닙에 의한 세포 사멸에서 mTOR의 중요성을 확인하였다. 아파티닙은 1세대 TKI인 게피티닙에 비해 구강암 세포주에서 더 우수한 항증식 및 사멸 촉진 효과를 나타내었으며, Mcl-1 단백질 발현을 효과적으로 감소시켰다. 또한, HSC-3 세포주를 이식한 xenograft model에서 아파티닙의 항암활성이 확인되었다.

결론: 본 연구의 결과를 통해 아파티닙이 EGFR/mTOR/Mcl-1 신호전달경로를 조절함으로써 구강암에서 세포 사멸을 유도한다는 것을 확인하였고, 이는 아파티닙이 구강암 치료를 위한 효과적인 항암 화학요법 후보물질로서 가능성이 있음을 제시한다.

주요어: 구강암, 아파티닙, 세포사멸, EGFR, Mcl-1, mTOR

학 번: 2019-36435